LETTER

doi:10.1038/nature18310

Coordinating cardiomyocyte interactions to direct ventricular chamber morphogenesis

Peidong Han[1], Joshua Bloomekatz[1], Jie Ren[1], Ruilin Zhang[1], Jonathan D. Grinstein[1], Long Zhao[2], C. Geoffrey Burns[2], Caroline E. Burns[2], Ryan M. Anderson[3] & Neil C. Chi[1,4]

Many organs are composed of complex tissue walls that are structurally organized to optimize organ function. In particular, the ventricular myocardial wall of the heart comprises an outer compact layer that concentrically encircles the ridge-like inner trabecular layer. Although disruption in the morphogenesis of this myocardial wall can lead to various forms of congenital heart disease[1] and non-compaction cardiomyopathies[2], it remains unclear how embryonic cardiomyocytes assemble to form ventricular wall layers of appropriate spatial dimensions and myocardial mass. Here we use advanced genetic and imaging tools in zebrafish to reveal an interplay between myocardial Notch and Erbb2 signalling that directs the spatial allocation of myocardial cells to their proper morphological positions in the ventricular wall. Although previous studies have shown that endocardial Notch signalling non-cell-autonomously promotes myocardial trabeculation through Erbb2 and bone morphogenetic protein (BMP) signalling[3], we discover that distinct ventricular cardiomyocyte clusters exhibit myocardial Notch activity that cell-autonomously inhibits Erbb2 signalling and prevents cardiomyocyte sprouting and trabeculation. Myocardial-specific Notch inactivation leads to ventricles of reduced size and increased wall thickness because of excessive trabeculae, whereas widespread myocardial Notch activity results in ventricles of increased size with a single-cell-thick wall but no trabeculae. Notably, this myocardial Notch signalling is activated non-cell-autonomously by neighbouring Erbb2-activated cardiomyocytes that sprout and form nascent trabeculae. Thus, these findings support an interactive cellular feedback process that guides the assembly of cardiomyocytes to morphologically create the ventricular myocardial wall and more broadly provide insight into the cellular dynamics of how diverse cell lineages organize to create form.

The embryonic zebrafish heart comprises 200–300 cardiomyocytes when cardiac chambers form[4], and thus provides an opportunity to interrogate in detail how individual cardiomyocytes organize to create the nascent structures of the vertebrate embryonic ventricular wall. As a result, previous zebrafish studies have shown that distinct cardiomyocytes extend from the embryonic ventricular wall into the lumen to develop cardiac trabeculae[5], whereas others remain within this outer wall to create the primordial layer[4]. Yet, how these cardiomyocytes are selected to form the distinct myocardial layers of the ventricular wall remains to be fully elucidated.

Because of the role of Notch signalling in regulating cell–cell interactions[6,7], we examined its dynamic activation during zebrafish embryonic ventricular morphogenesis using the *Tg(Tp1:d2GFP)* Notch reporter line, which expresses a destabilized green fluorescent protein upon Notch activation[8] (Fig. 1 and Extended Data Fig. 1). As previously reported[9], we observed Notch signalling first in the ventricular endocardium at 24 hours post-fertilization (hpf), which then becomes restricted to the atrioventricular (AV) and outflow tract (OFT) endocardium at 48 hpf (Extended Data Fig. 1a–l). From 72 to 96 hpf when cardiac trabeculation initiates[5,10,11], a subset of ventricular cardiomyocytes begins to express Notch-activated *Tp1*:d2GFP and remains

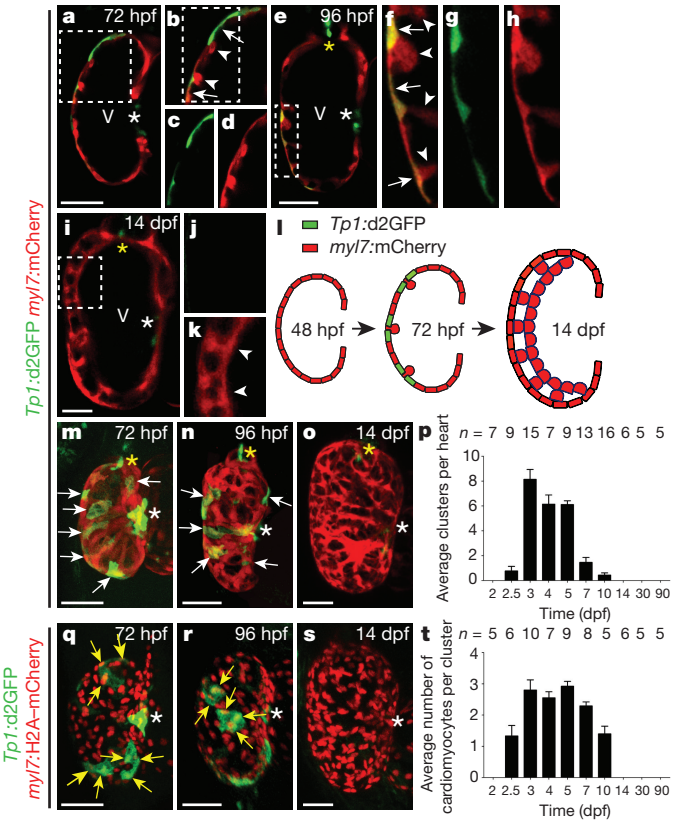

Figure 1 | Notch signalling is dynamically activated in distinct myocardial clusters during cardiac morphogenesis. Cardiac ventricles at 72 hpf, 96 hpf, and 14 dpf expressing (**a**–**k**, **m**–**o**) *Tp1*:d2GFP; *myl7*:mCherry or (**q**–**s**) *Tp1*:d2GFP; *myl7*:H2A–mCherry. **a**–**k**, Confocal slices; **m**–**o**, **q**–**s**, three-dimensional reconstructions. **b**, **c**–**d**, **f**–**h**, **j**–**k**, Magnifications of boxed areas in **a**, **b**, **e**, and **i**, respectively. Images **c** and **d**, **g** and **h**, and **j** and **k** are single channels from **b**, **f**, and **i** merged images, respectively. **l**, Schematic of myocardial Notch signalling. **p**, **t**, Quantification of (**p**) myocardial *Tp1*:d2GFP$^+$ clusters and (**t**) cardiomyocytes per *Tp1*:d2GFP$^+$ cluster. *n*, Number of embryos analysed per stage. White arrows, *Tp1*:d2GFP$^+$ cardiomyocytes; white arrowheads, trabeculating cardiomyocytes; yellow arrows, cardiomyocytes in *Tp1*:d2GFP$^+$ clusters. White and yellow asterisks, AV and OFT. Mean ± s.e.m. Scale bar, 25 μm.

[1]Department of Medicine, Division of Cardiology, University of California, San Diego, La Jolla, California 92093, USA. [2]Cardiovascular Research Center, Division of Cardiology, Department of Medicine, Massachusetts General Hospital and Harvard Medical School, Charlestown, Massachusetts 02129, USA. [3]Center for Diabetes and Metabolic Diseases, Department of Pediatrics and Department of Cellular and Integrative Physiology, Indiana University School of Medicine, Indianapolis, Indiana 46202, USA. [4]Institute of Genomic Medicine, University of California, San Diego, La Jolla, California 92093, USA.

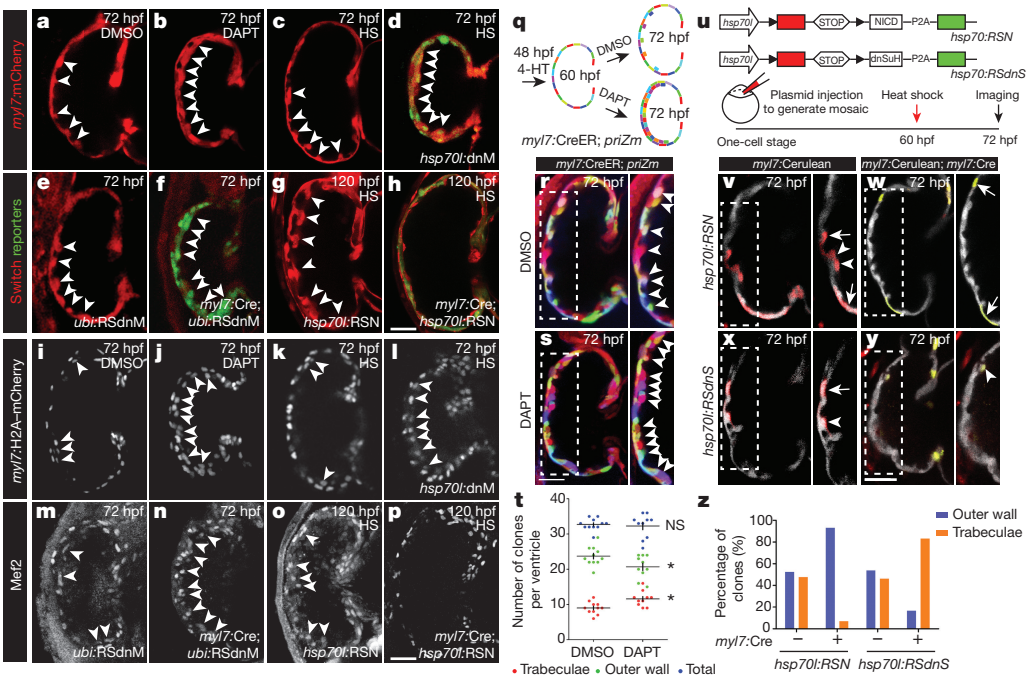

Figure 2 | Myocardial Notch signalling cell-autonomously regulates cardiomyocyte segregation between ventricular wall layers. Inhibiting Notch signalling by (**b**, **j**) DAPT treatment, (**d**, **l**) global dnMAML–GFP (*hsp70l*:dnM), or (**f**, **n**) myocardial-specific dnMAML expression (*myl7*:Cre; *ubi*:RSdnM) leads to excessive trabeculation at 72 hpf, whereas (**h**, **p**) myocardial-specific constitutive Notch activation via NICD expression (*myl7*:Cre; *hsp70l*:RSN) diminishes trabeculation at 120 hpf. **a**, **c**, **e**, **g**, **i**, **k**, **m**, **o**, Respective controls for each condition. **a**–**p**, For quantification see Extended Data Fig. 5. **q**, Myocardial *priZm* (brainbow) clonal studies. **r**, **s**, The 72 hpf *myl7*:CreER; *priZm* myocardial clones treated with DMSO or DAPT at 60 hpf. **t**, Although DMSO- and DAPT-treated ventricles display a similar overall number of myocardial clones (blue) ($n = 10$ and 11 embryos), DAPT-treated ventricles exhibit more clones in trabeculae (red) and fewer in the outer ventricular wall (green), compared with control. Crosses, mean and s.e.m. $^*P < 0.05$, by Student's *t*-test. NS, not significant. **u**, Notch-altering mosaic cardiomyocyte studies. **w**, Constitutively activated Notch cardiomyocytes expressing NICD-P2A–Emerald are primarily located on the ventricular outer wall ($n = 13/14$ clones, Fisher's exact test, $P < 0.05$); whereas (**y**) Notch-inhibited cardiomyocytes expressing dnSuH-P2A–Emerald are mainly found in trabeculae ($n = 15/18$ clones, Fisher's exact test, $P < 0.05$). **v**, **x**, In controls lacking *Tg(myl7:cre)*, mCherry$^+$ cardiomyocytes are distributed equally between both layers ($n = 11/21$ and 14/26 clones in the outer wall). **z**, Quantitative analysis of **v**–**y**. Insets are magnifications of boxed areas. Arrowheads and arrows, trabeculae and outer wall cardiomyocytes. HS, heat shock. Scale bar, 25 μm.

in the ventricular outer wall (Fig. 1a–h, arrows, and Extended Data Fig. 1m–o, arrows), whereas ventricular cardiomyocytes extending to form cardiac trabeculae fail to express *Tp1*:d2GFP (Fig. 1a–h arrowheads). These *Tp1*:d2GFP$^+$ cardiomyocytes are frequently adjacent to sprouting *Tp1*:d2GFP$^-$ cardiomyocytes (Fig. 1a–h) and form clusters of two or three cardiomyocytes across the surface of the ventricular myocardial wall (Fig. 1m–t), which quantitatively correlate with the number of emerging cardiac trabeculae (Extended Data Fig. 1p–r). However, after the heart has established cardiac trabeculae, these *Tp1*:d2GFP$^+$ myocardial clusters progressively decrease and are no longer observed by 14 days post-fertilization (dpf), despite the presence of *Tp1*:d2GFP$^+$ AV and OFT endocardial cells (Fig. 1i–l, o, p, s, t and Extended Data Fig. 1s, t).

Using the *Tg(Tp1:eGFP)* Notch reporter line[12], which expresses a more stable fluorescent protein than *Tg(Tp1:d2GFP)* (Extended Data Fig. 2a–h), we observed that *Tp1*:eGFP$^+$ cardiomyocytes remain present in the ventricular outer wall until 30–45 dpf because of the eGFP perdurance, and then become the ventricular primordial layer by 60–90 dpf when the ventricular cortical layer of the adult zebrafish heart forms[4] (Extended Data Fig. 3a–n). Unlike ventricular trabecular and cortical cardiomyocytes, these *Tp1*:eGFP$^+$ ventricular primordial cardiomyocytes fail to display organized sarcomeres by α-actinin immunostaining, are surrounded by extensive wheat germ agglutinin stained extracellular matrix and exhibit a thin cellular morphology as previously reported[4] (Extended Data Fig. 3o–t). Overall, these data suggest that early myocardial Notch signalling may determine which ventricular cardiomyocytes remain in the embryonic ventricular outer wall to subsequently become the distinctive ventricular primordial layer of the adult zebrafish heart.

We next investigated the role of Notch signalling in the endocardium and myocardium during ventricular morphogenesis through selectively perturbing Notch signalling at specific cardiac developmental stages. Treating zebrafish embryos with DAPT, which effectively decreases *Tp1*:d2GFP Notch reporter expression and inhibits Notch signalling (Extended Data Fig. 2), from 20 to 48 hpf when Notch signalling is activated in the endocardium, reduces cardiac trabeculation (Extended Data Fig. 2q–s) as previously described[3]; however, treating from 60 to 72 hpf, when Notch signalling is present in the ventricular myocardium, results in increased trabeculae formation (Fig. 2a, b, i, j). Consistent with these results, BMP signalling, which is activated in ventricular trabeculae[3], is also increased in similarly DAPT-treated zebrafish embryos from 60 to 72 hpf (Extended Data Fig. 4a–f). Furthermore, heat-shocking *Tg(hsp70l:dnMAML–GFP)*[13] (abbreviated as *hsp70l:dnM*) embryos from 60 to 72 hpf, which induces dominant negative Mastermind-like (dnMAML) expression to block downstream Notch signalling, results in similar excessive trabeculation (Fig. 2c, d, k, l).

To explore whether Notch signalling functions in a cardiomyocyte-specific manner to directly guide myocardial cell fate position within the ventricle, we employed a myocardial-specific Cre (Extended Data Fig. 5a–d) strategy in combination with *Tg(ubi:loxp-mKate2-STOP-loxp-dnMAML–GFP)* or *Tg(hsp70l:loxp–mCherry–STOP-loxp-NICD-P2A–Emerald)*[14] 'switch lines' (abbreviated as *ubi:RSdnM* and *hsp70l:RSN*) to inhibit or activate Notch signalling in cardiomyocytes, respectively. As observed in DAPT-treated and heat-shocked *Tg(hsp70l:dnM)* zebrafish from 60 to 72 hpf, *Tg(myl7:Cre; ubi:RSdnM)* zebrafish display excessive cardiac trabeculation due to inhibition of myocardial Notch signalling (Fig. 2e, f, m, n). Conversely,

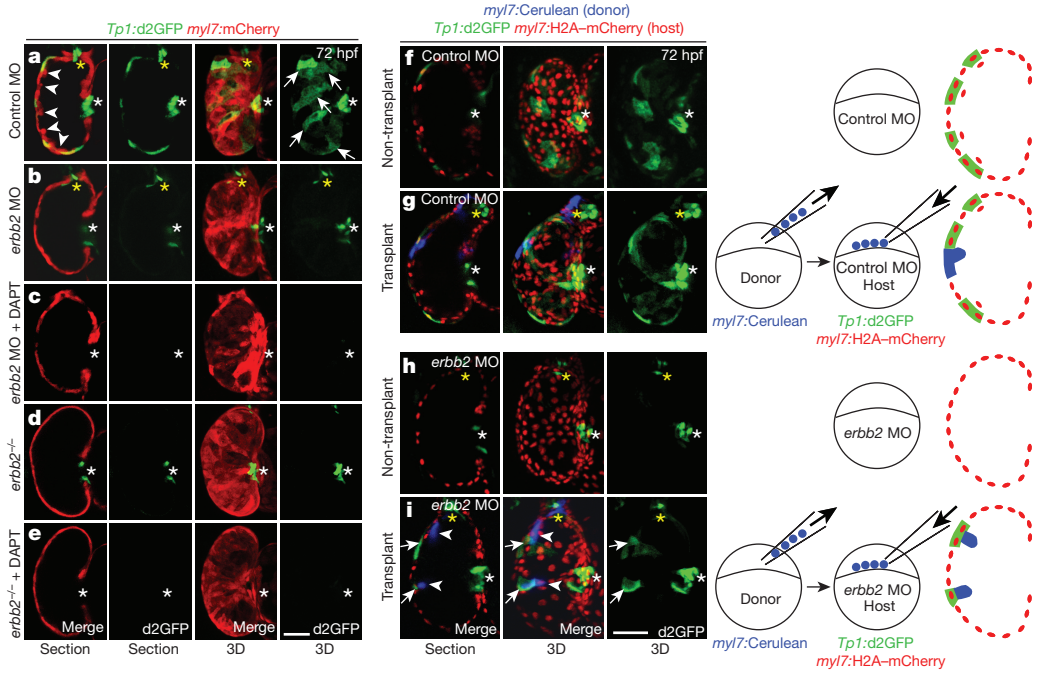

Figure 3 | Myocardial Erbb2 signalling non-cell-autonomously activates Notch signalling in neighbouring cardiomyocytes. Compared with (**a**) controls ($n = 0/15$ embryos), *Tp1*:d2GFP; *myl7*:mCherry (**b**) *erbb2* MO ($n = 10/12$) and (**d**) *erbb2*$^{-/-}$ mutants ($n = 10/10$) display reduced trabeculae and myocardial Notch signalling. **c**, **e**, DAPT treatment at 60 hpf cannot rescue these myocardial defects, but can diminish AV and OFT endocardial Notch signalling (asterisks) ($n = 15/17$, $17/17$ embryos, respectively). **f**–**i**, Blastomere transplantation studies. Compared with (**g**) control MO hosts ($n = 12$ embryos), (**i**) a greater percentage of donor *Tg(myl7:Cerulean)* wild-type cardiomyocytes are located in the trabeculae of *erbb2* MO *Tg(Tp1:d2GFP; myl7:H2A–mCherry)* hosts ($n = 10$). In contrast to (**h**) non-transplanted *erbb2* MO hearts ($n = 16$), (**i**) transplanted donor *Tg(myl7:Cerulean)* wild-type cardiomyocytes (arrowheads) can activate myocardial Notch activity (*Tp1*:d2GFP) in neighbouring *erbb2* MO *Tg(Tp1:d2GFP; myl7:H2A–mCherry)* host cardiomyocytes (arrows, $n = 10$). Scale bar, 25 μm.

heat-shocking *Tg(myl7:Cre; hsp70l:RSN)* zebrafish, which induces myocardial Notch-intracellular domain (NICD) expression, between 60 and 120 hpf leads to cardiac ventricles without significant trabeculae because of constitutively activated Notch signalling throughout the myocardium (Fig. 2g, h, o, p). Moreover, constitutive myocardial Notch activation at later time points (80, 96, and 120 hpf to 7 dpf) prevents trabeculae from further sprouting and/or extending (Extended Data Fig. 6a–g); however, trabeculae continue to develop after the cessation of this myocardial Notch activity, but fail to recover to wild-type levels (Extended Data Fig. 6h, i).

In line with these findings, we discovered that Notch inhibition results in smaller ventricular areas (Fig. 2a–f and Extended Data Fig. 5e) and thicker ventricular myocardial walls (Fig. 2a–f and Extended Data Fig. 5f) due to increased cardiomyocytes within the trabecular layer (approximately two or three cells thick) (Fig. 2i–n, Extended Data Fig. 5g), whereas Notch activation gives rise to larger ventricular areas (Fig. 2g, h, Extended Data Fig. 5e) and thinner ventricular myocardial walls (Fig. 2g, h and Extended Data Fig. 5f) that are about one cell thick with no apparent trabecular cardiomyocytes (Fig. 2o, p and Extended Data Fig. 5g). Although these hearts do not exhibit a significant difference in overall cardiomyocyte numbers compared with control hearts (Extended Data Fig. 5h–p), we did discover that Notch inhibition promotes the redistribution of N-cadherin away from intercellular contacts whereas Notch activation prevents this reorganization (Extended Data Fig. 7), suggesting that myocardial Notch signalling may control ventricular size and wall thickness through regulating the allocation of cardiomyocytes between the ventricular wall layers via cell–cell contacts. To further investigate this possibility, we monitored the fate of individual genetically labelled cardiomyocytes using a myocardial specific Brainbow system *Tg(myl7:CreER; priZm)*[4] (Fig. 2q–t). After confirming that adjacent cardiomyocytes were consistently labelled with different colours at 60 hpf before trabeculation (Extended Data Fig. 8), we treated zebrafish embryos with DAPT or dimethylsulfoxide (DMSO) from 60 to 72 hpf. DAPT treatment leads to increased numbers of trabeculating clones and conversely decreased numbers of non-trabeculating clones compared with DMSO-treated hearts; however, the total number of ventricular cardiomyocyte clones is not significantly different (Fig. 2r–t), further supporting the idea that Notch signalling segregates individual cardiomyocyte clones between the ventricular outer wall and inner trabecular layers.

To examine whether Notch signalling acts cell-autonomously to control cardiomyocyte sprouting, we perturbed Notch signalling in individual cardiomyocytes during trabeculation by injecting *hsp70l:loxp–mCherry–STOP-loxp-NICD-P2A–Emerald* (*hsp70l:RSN*, Notch activating) or *hsp70l:loxp–mCherry–STOP-loxp-dnSuH-P2A–Emerald*[15] (*hsp70l:RSdnS*, dominant negative Suppressor of Hairless/Notch repressing) switch plasmids into *Tg(myl7:Cerulean)*[16]; *Tg(myl7:Cre)* zebrafish embryos (Fig. 2u). Heat-shocking these injected fish from 60 to 72 hpf resulted in most Notch-activated NICD-P2A–Emerald^{+} cardiomyocytes remaining in the ventricular outer myocardial wall (Fig. 2w, z), whereas Notch-inhibited dnSuH-P2A–Emerald^{+} cardiomyocytes reside primarily in trabeculae (Fig. 2y, z). Heat-shocking injected control fish lacking *Tg(myl7:Cre)* generated mCherry^{+} cardiomyocytes that were distributed equally between both myocardial layers (Fig. 2v, x, z), altogether revealing a myocardial cell-autonomous role for Notch signalling.

Because Neuregulin/Erbb2 and BMP10 signalling can promote cardiac trabeculation[3,10,17], we investigated whether myocardial Notch may cross-talk with these signalling pathways to regulate cardiomyocyte selection between the ventricular wall layers. Inhibiting Erbb2 signalling with AG1478 treatment[10] from 60 to 72 hpf prevents cardiac trabeculation and expression of *Tp1*:d2GFP in cardiomyocytes, although *Tp1*:d2GFP remains expressed in AV and OFT endocardial cells (Extended Data Fig. 9a, b). Consistent with these findings, both *erbb2* morpholino (MO) knockdown and *erbb2*$^{-/-}$ mutant (*erbb2*^{st50}) *Tg(Tp1:d2GFP)* embryos, which exhibit similar trabecular defects[10,18],

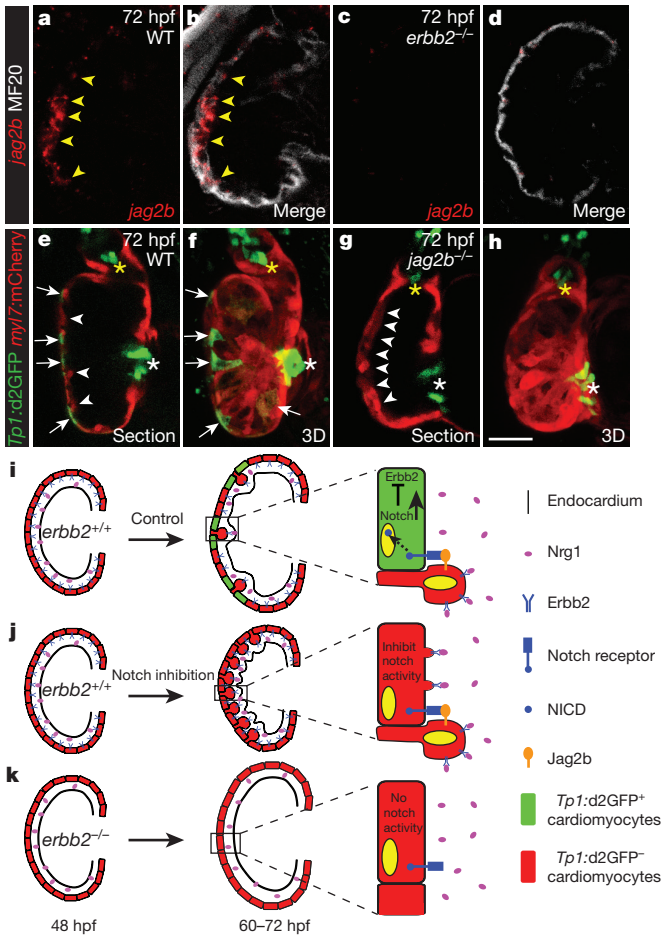

Figure 4 | The Notch ligand Jag2b mediates cooperative interactions between cardiomyocytes. a–d, Ventricular myocardial (MF20^{+}) *jag2b* is expressed in (**a**, **b**) wild-type (WT) ($n = 6/6$ embryos) but not (**c**, **d**) *erbb2*$^{-/-}$ mutant hearts ($n = 0/5$). **e–h**, Compared with (**e**, **f**) WT controls ($n = 0/10$), (**g**, **h**) *Tg(Tp1:d2GFP; myl7:mCherry) jag2b*$^{-/-}$ mutants exhibit increased trabeculation and reduced myocardial Notch signalling at 72 hpf ($n = 8/8$). Yellow arrowheads, *jag2b*$^{+}$ cardiomyocytes; white arrowheads, trabeculae; white arrows, *Tp1*:d2GFP^{+} cardiomyocytes; white and yellow asterisks, AV and OFT. Scale bar, 25 μm. Myocardial Notch signalling model: (**i**) endocardial Neuregulin/Nrg1 activates myocardial Erbb2 signalling, which cell-autonomously triggers myocardial sprouting and Jag2b expression (60–72 hpf). Jag2b activates Notch signalling in neighbouring cardiomyocytes, which cell-autonomously inhibits *erbb2* expression and trabeculae formation (magnified area). **j**, Inhibiting Notch signalling allows all cardiomyocytes to express *erbb2*, respond to Neuregulin, and sprout and form trabeculae. **k**, Blocking Erbb2 signalling prevents trabeculation, Jag2b expression, and Notch activation in neighbouring cardiomyocytes.

also fail to display Notch reporter expression in the myocardium (Fig. 3a, b, d), supporting a requirement for Erbb2 signalling in the initiation of trabeculation and the activation of myocardial Notch signalling. Notably, neither DAPT treatment nor heat-shock induction of dnMAML between 60 and 72 hpf, which alone increases trabeculation (Fig. 2), could rescue the relative lack of cardiac trabeculae in zebrafish with loss of Erbb2 function (Fig. 3c, e and Extended Data Fig. 9b–e). In contrast to the Erbb2 loss of function findings, embryos treated with Dorsomorphin[19] from 60 to 72 hpf to inhibit BMP signalling still form cardiac trabeculae and express *Tp1*:d2GFP in the outer myocardial wall (Extended Data Fig. 4m–p) despite the abrogation of the BMP-reporter signal (*BRE*:d2GFP) in the trabecular layer (Extended Data Fig. 4j–l). However, by 7 dpf, these hearts display aberrant and stunted cardiac trabeculae compared with DMSO-treated fish (Extended Data Fig. 4q–s), corroborating a requirement for BMP signalling in the maintenance but not the initiation of cardiac trabeculation[20].

To explore whether Notch activation negatively regulates Erbb2 signalling to prevent trabeculae formation, we examined *erbb2* expression in 72 hpf *Tp1*:d2GFP hearts and discovered that *erbb2* is expressed in many ventricular cardiomyocytes but diminished in *Tp1*:d2GFP^{+} cardiomyocytes (Extended Data Fig. 9f–j). In support of these findings, constitutive myocardial Notch activation by heat-shocking *Tg(myl7:Cre; hsp70l:RSN)* fish between 60 and 120 hpf results in the dramatic reduction of *erbb2* myocardial expression (Extended Data Fig. 9k, l, o, p). In contrast, Notch-inhibited hearts treated with DAPT from 60 to 72 hpf exhibit increased *erbb2* myocardial expression (Extended Data Fig. 9m, n, q, r). Thus, myocardial Notch signalling may block Neuregulin/Erbb2 signalling by downregulating *erbb2* expression to inhibit cardiomyocyte sprouting.

Since Notch signalling has been shown to mediate cell fate position through lateral inhibition mechanisms[6,7,21,22], we investigated whether Erbb2 signalling non-cell-autonomously activates myocardial Notch signalling in neighbouring cardiomyocytes. Thus, we created mosaic embryos by transplanting *Tg(myl7:Cerulean)* wild-type donor blastomeres into *erbb2* or control MO injected *Tg(Tp1:d2GFP); Tg(myl7:H2A–mCherry)*[23] host embryos and assessed the ability of wild-type donor cells to contribute to the ventricular wall layers and activate myocardial Notch signalling. As previously reported[10], a greater percentage of donor-derived wild-type cardiomyocytes is present in the trabeculae of *erbb2* knockdown embryos compared with control embryos (compare Fig. 3i with Fig. 3g; Extended Data Fig. 10a). Although non-transplanted *erbb2* knockdown hearts fail to exhibit myocardial Notch activity (Fig. 3f, h), transplanted *erbb2* knockdown host hearts containing wild-type donor myocardial cells (*myl7*:Cerulean^{+}) can activate myocardial *Tp1*:d2GFP expression (Fig. 3i and Extended Data Fig. 10b). Upon closer inspection, these host *erbb2* knockdown *Tp1*:d2GFP^{+} cardiomyocytes (Fig. 3i, arrows) appear adjacent to donor wild-type *myl7*:Cerulean^{+} cardiomyocytes (Fig. 3i, arrowheads, and Extended Data Fig. 10c), supporting a role for Erbb2-responsive cardiomyocytes in activating Notch signalling in neighbouring cardiomyocytes.

On the basis of these results, we searched for potential Notch ligands mediating the activation of Notch signalling in neighbouring cardiomyocytes and discovered that *jag2b* is expressed in select ventricular cardiomyocytes at 72 hpf when myocardial Notch signalling is activated (Fig. 4a, b). This ventricular myocardial *jag2b* expression is reduced in *erbb2*$^{-/-}$ mutant hearts (Fig. 4c, d), suggesting that Erbb2 signalling may activate Notch signalling in neighbouring cardiomyocytes through *jag2b*. In support of this possibility, we discovered that *jag2b*$^{-/-}$ mutant hearts exhibit not only increased trabeculation as observed in Notch-inhibited hearts but also reduced *Tp1*:d2GFP Notch reporter activity in the ventricular myocardium but not in the AV or OFT endocardium (Fig. 4e–h). Together these data support a model in which myocardial Erbb2 signalling non-cell-autonomously activates Notch signalling in neighbouring ventricular outer-wall cardiomyocytes through Jag2b, which in turn leads to the reduction of *erbb2* expression, subsequent inhibition of Erbb2 signalling, and suppression of cardiomyocyte sprouting (Fig. 4i–k).

Overall, these findings reveal a molecular mechanism whereby Notch and Erbb2 signalling coordinates social cellular interactions between cardiomyocytes that determine their morphological fate within the ventricular wall. Although previous studies have suggested that Notch signalling may be activated in the myocardium[24–27], our zebrafish studies illuminate the precise role of myocardial Notch activity in forming the ventricular wall. Similar to the receptor tyrosine kinase (RTK)-Notch lateral inhibition signalling mechanisms that regulate epithelial tip and stalk cell formation during branching morphogenesis[6,7], myocardial Notch acts in concert with the RTK Erbb2 to segregate embryonic cardiomyocytes into two functionally distinct classes of cells: (1) sprouting cardiomyocytes that respond to Neuregulin via

Erbb2 and (2) non-sprouting Notch-activated cardiomyocytes, in which Notch signalling inhibits *erbb2* expression. These roles appear not to be pre-specified, but rather are determined by social interactions between cardiomyocytes. Furthermore, recent studies have reported human Notch genetic variants linked to a wide spectrum of congenital heart diseases including non-compaction cardiomyopathies[28,29], which exhibit similar severe ventricular wall defects to those observed in our Notch studies. More broadly, our studies support a conserved role for intercellular cross-talk between RTKs and Notch signalling for allocating cells within organ substructures and might be particularly relevant in developing strategies for human pluripotent stem-cell tissue-specific developmental and disease modelling or regenerative therapies.

Online Content Methods, along with any additional Extended Data display items and Source Data, are available in the online version of the paper; references unique to these sections appear only in the online paper.

Received 24 September 2015; accepted 5 May 2016.

1. Fahed, A. C., Gelb, B. D., Seidman, J. G. & Seidman, C. E. Genetics of congenital heart disease: the glass half empty. *Circ. Res.* **112,** 707–720 (2013).
2. Zemrak, F. *et al.* The relationship of left ventricular trabeculation to ventricular function and structure over a 9.5-year follow-up: the MESA study. *J. Am. Coll. Cardiol.* **64,** 1971–1980 (2014).
3. Grego-Bessa, J. *et al.* Notch signaling is essential for ventricular chamber development. *Dev. Cell* **12,** 415–429 (2007).
4. Gupta, V. & Poss, K. D. Clonally dominant cardiomyocytes direct heart morphogenesis. *Nature* **484,** 479–484 (2012).
5. Staudt, D. W. *et al.* High-resolution imaging of cardiomyocyte behavior reveals two distinct steps in ventricular trabeculation. *Development* **141,** 585–593 (2014).
6. Ghabrial, A. S. & Krasnow, M. A. Social interactions among epithelial cells during tracheal branching morphogenesis. *Nature* **441,** 746–749 (2006).
7. Siekmann, A. F. & Lawson, N. D. Notch signalling limits angiogenic cell behaviour in developing zebrafish arteries. *Nature* **445,** 781–784 (2007).
8. Clark, B. S. *et al.* Loss of Llgl1 in retinal neuroepithelia reveals links between apical domain size, Notch activity and neurogenesis. *Development* **139,** 1599–1610 (2012).
9. Samsa, L. A. *et al.* Cardiac contraction activates endocardial Notch signaling to modulate chamber maturation in zebrafish. *Development* **142,** 4080–4091 (2015).
10. Liu, J. *et al.* A dual role for ErbB2 signaling in cardiac trabeculation. *Development* **137,** 3867–3875 (2010).
11. Ong, L. L., Kim, N., Mima, T., Cohen-Gould, L. & Mikawa, T. Trabecular myocytes of the embryonic heart require N-cadherin for migratory unit identity. *Dev. Biol.* **193,** 1–9 (1998).
12. Parsons, M. J. *et al.* Notch-responsive cells initiate the secondary transition in larval zebrafish pancreas. *Mech. Dev.* **126,** 898–912 (2009).
13. Zhao, L. *et al.* Notch signaling regulates cardiomyocyte proliferation during zebrafish heart regeneration. *Proc. Natl Acad. Sci. USA* **111,** 1403–1408 (2014).
14. Anderson, R. M. *et al.* Hepatocyte growth factor signaling in intrapancreatic ductal cells drives pancreatic morphogenesis. *PLoS Genet.* **9,** e1003650 (2013).
15. Ninov, N., Borius, M. & Stainier, D. Y. Different levels of Notch signaling regulate quiescence, renewal and differentiation in pancreatic endocrine progenitors. *Development* **139,** 1557–1567 (2012).
16. Mathews, E. S. *et al.* Mutation of 3-hydroxy-3-methylglutaryl CoA synthase I reveals requirements for isoprenoid and cholesterol synthesis in oligodendrocyte migration arrest, axon wrapping, and myelin gene expression. *J. Neurosci.* **34,** 3402–3412 (2014).
17. Peshkovsky, C., Totong, R. & Yelon, D. Dependence of cardiac trabeculation on neuregulin signaling and blood flow in zebrafish. *Dev. Dyn.* **240,** 446–456 (2011).
18. Lyons, D. A. *et al.* erbb3 and erbb2 are essential for Schwann cell migration and myelination in zebrafish. *Curr. Biol.* **15,** 513–524 (2005).
19. Collery, R. F. & Link, B. A. Dynamic smad-mediated BMP signaling revealed through transgenic zebrafish. *Dev. Dyn.* **240,** 712–722 (2011).
20. Chen, H. *et al.* BMP10 is essential for maintaining cardiac growth during murine cardiogenesis. *Development* **131,** 2219–2231 (2004).
21. Sternberg, P. W. Lateral inhibition during vulval induction in *Caenorhabditis elegans*. *Nature* **335,** 551–554 (1988).
22. Heitzler, P. & Simpson, P. The choice of cell fate in the epidermis of *Drosophila*. *Cell* **64,** 1083–1092 (1991).
23. Schumacher, J. A., Bloomekatz, J., Garavito-Aguilar, Z. V. & Yelon, D. *tal1* regulates the formation of intercellular junctions and the maintenance of identity in the endocardium. *Dev. Biol.* **383,** 214–226 (2013).
24. Rentschler, S. *et al.* Notch signaling regulates murine atrioventricular conduction and the formation of accessory pathways. *J. Clin. Invest.* **121,** 525–533 (2011).
25. Zhao, C. *et al.* Numb family proteins are essential for cardiac morphogenesis and progenitor differentiation. *Development* **141,** 281–295 (2014).
26. Yang, J. *et al.* Inhibition of Notch2 by Numb/Numblike controls myocardial compaction in the heart. *Cardiovasc. Res.* **96,** 276–285 (2012).
27. Leimeister, C., Externbrink, A., Klamt, B. & Gessler, M. Hey genes: a novel subfamily of hairy- and Enhancer of split related genes specifically expressed during mouse embryogenesis. *Mech. Dev.* **85,** 173–177 (1999).
28. Li, L. *et al.* Alagille syndrome is caused by mutations in human Jagged1, which encodes a ligand for Notch1. *Nature Genet.* **16,** 243–251 (1997).
29. Luxán, G. *et al.* Mutations in the NOTCH pathway regulator MIB1 cause left ventricular noncompaction cardiomyopathy. *Nature Med.* **19,** 193–201 (2013).

Acknowledgements We thank N. Tedeschi for fish care; B. Le for experimental assistance; S. Evans, D. Yelon, and Chi laboratory members for comments on the manuscript; N. Ninov and D. Stainier for plasmids; B. Link for the d2GFP BMP and d2GFP Notch reporter lines; N. Lawson for the eGFP Notch reporter line; B. Appel for the myocardial Cerulean line; K. Poss for the myocardial CreER and Brainbow/priZm lines; and W. Talbot for the *erbb2* mutant. This work was supported in part by grants from American Heart Association (14POST20380738) to L.Z.; the March of Dimes (1-FY14-327) to R.A.M.; the NIH/NHLBI (5R01HL127067) to C.G.B. and C.E.B.; and the National Institutes of Health to N.C.C.

Author Contributions P.H. and N.C.C. conceived the project and the design of the experimental strategy. P.H., J.R., J.B., R.Z., and J.D.G. conducted experiments. L.Z. generated the *ubi:*RSdnM transgenic line. P.H. and N.C.C. generated and characterized the *myl7:*Cre transgenic line. C.E.B., C.G.B., and R.A.M. provided key reagents. P.H., J.B. and N.C.C. prepared the manuscript.

Author Information Reprints and permission information is available at www.nature.com/reprints. The authors declare no competing financial interests. Correspondence and requests for materials should be addressed to N.C.C. (nchi@ucsd.edu).

Reviewer Information *Nature* thanks B. G. Bruneau and the other anonymous reviewer(s) for their contribution to the peer review of this work.

METHODS

Zebrafish husbandry and strains. Zebrafish (*Danio rerio*) were raised under standard laboratory conditions at 28 °C. All animal work was approved by the University of California at San Diego Institutional Animal Care and Use Committee. The following established transgenic and mutant lines were used: *Tg(EPV.Tp1-Mmu.Hbb:d2GFP)*^{mw43} (ref. 8) abbreviated as *Tg(Tp1:d2GFP)*; *Tg(EPV.Tp1-Mmu.Hbb:eGFP)*^{um14} (ref. 12) abbreviated as *Tg(Tp1:eGFP)*; *Tg(BRE-AAVmlp:d2GFP)*^{mw30} (ref. 19) abbreviated as *Tg(BRE:d2GFP)*; *Tg(hsp70l:dnMAML-GFP)*^{fb10} (ref. 13) abbreviated as *Tg(hsp70l:dnM)*; *Tg(kdrl:ras–mCherry)*^{S896} (ref. 30); *Tg(myl7:H2A–mCherry)*^{sd12} (ref. 23); *Tg(myl7:mCherry)*^{sd7} (ref. 31); *Tg(myl7:Cerulean)*^{co19} (ref. 16); *Tg(myl7:eGFP–HRAS)*^{s883} (ref. 32) abbreviated as *Tg(myl7:ras–eGFP)*; *Tg(myl7:CreER)*^{pd10} (ref. 33); *Tg(β-act2:Brainbow1.0L)*^{pd49} (ref. 4) abbreviated as *Tg(priZm)*; *Tg(hsp70l:loxp–mCherry–STOP-loxp-NICD-P2A–Emerald)*^{S961} (ref. 14) abbreviated as *Tg(hsp70l:RSN)*; *Tg(β-act2:loxP-DsRed-STOP-loxP–eGFP)*^{s928} (ref. 33) abbreviated as *Tg* (ref. *β-act2:RSG)*; *erbb2*^{st50} (ref. 18), and *jag2b*^{hu3425} (ref. 34).

To generate the *Tg(myl7:Cre)*^{sd38} transgenic line, a 900-base-pair fragment of the *myl7* promoter[35] was cloned upstream of the *Cre* recombinase gene into a multi-cloning site flanked by I-SceI sites in the pBluescript-SK vector. Standard I-SceI meganuclease transgenesis[36] was used to create transgenic founders which were screened for myocardial Cre recombinase activity by crossing to the *Tg(β-act2:RSG)*^{s928} line. Three independent founders were identified, all with similar levels of Cre recombinase activity and matching the expression of *Tg(myl7:Cerulean)*^{co19} (Extended Data Fig. 5a–d). A single representative founder was propagated further.

To generate the *Tg(ubi:loxp-mKate2-STOP-loxp-dnMAML–GFP)*^{fb16} strain, abbreviated as *Tg(ubi:RSdnM)*, gateway cloning technology (Life Technologies) was used to conduct an LR recombination reaction with the *pENTR5′_ubi*[37], *pME-loxp-mKate2-STOP-loxp*, *p3E-dnMAML–GFP* entry vectors and the *pDESTol2pA2* destination vector[38]. The *pME-loxp-mKate2-STOP-loxp* entry vector was created by replacing the *AmCyan* complementary DNA in the *pME-loxp-AmCyan-STOP-loxp*[39] vector with a complementary DNA encoding mKate2 (Evrogen) using In-Fusion HD cloning (Clontech Laboratories). The *p3E-dnMAML–GFP* entry vector was generated by conducting a BP recombination reaction between a PCR product encoding a fusion protein between dnMAML and GFP amplified from *pME-dnMAML–GFP*[13] and the Gateway Donor Vector *pDONRP2R-P3*. Altogether the *ubi:loxp-mKate2-STOP-loxp-dnMAML–GFP* construct was co-injected with Tol2 transposase mRNA[38] into one-cell stage embryos to generate independent founders which were screened for mKate2 and then GFP upon Cre-mediated recombination. Founders with both mKate2 and GFP were propagated further.

Embryonic immunofluorescence and live imaging studies. Wholemount immunofluorescence studies were performed as previously described[40], with the following modifications. After initial fixation, any pre-existing fluorescence was quenched by incubating embryos in 2 M HCl at 37 °C for 30 min and washing with double-distilled H_2O and phosphate buffer saline with 0.1% Tween-20 (PBST). The antibodies used were anti-Mef2/C-21 (rabbit, Santa Cruz Biotechnology, 1:100), anti-MHC/MF20 (mouse, Developmental Studies Hybridoma Bank, 1:100) or anti-N-cadherin (rabbit, GeneTex, 1:100) followed by anti-rabbit IgG-Alexa 488 (goat, Life Technologies 1:200).

For embryonic studies of Notch activity, embryos containing the Notch reporters *Tg(Tp1:d2GFP)*^{mw43} or *Tg(Tp1:eGFP)*^{um14} in combination with myocardial-expressed transgenes such as *Tg(myl7:mCherry)*^{sd7} or endothelial expressed transgenes such as *Tg(kdrl:ras–mCherry)*^{S896} were imaged live[40]. The *Tp1* promoter used in these Notch reporter transgenics consists of 12 RPBJ-binding sites and reports Notch activity throughout the embryo as previously published[8,12]. These embryos were embedded in 1% low melting agarose (Lonza) in a coverslip bottom culture dish (MatTek) and cardiac contraction was arrested using Tricaine-S (Sigma MS-222) just before imaging.

To count the number of *Tp1:*d2GFP$^+$ clusters in each heart, we used three-dimensional reconstructions (Nikon NIS Elements software) from confocal stacks of *Tg(Tp1:d2GFP; myl7:mCherry)* embryos (5–16 hearts per stage). To count the number of cardiomyocytes per *Tp1:*d2GFP$^+$ cluster, *Tg(Tp1:d2GFP; myl7:H2A–mCherry)* embryos were used. Only cells expressing both H2A–mCherry and d2GFP were counted. We analysed five to ten hearts per stage to obtain the average number of cardiomyocytes in each *Tp1:*d2GFP cluster at each specified stage. Statistical analysis is described in the 'Image processing and statistical analysis' section below.

To assess the correlation between nascent trabeculae and *Tp1:*d2GFP$^+$ clusters at 72 hpf, trabeculae were identified in consecutive slices from a *Z*-stack and pseudo-coloured with magenta. A three-dimensional reconstruction was then used to generate the full view of the ventricle, where the number of nascent trabeculae and *Tp1:*d2GFP$^+$ clusters could be counted in each heart. These data are represented in a scatter plot (Extended Data Fig. 1r) and used to overlay a linear regression line.

Adult immunofluorescence and imaging studies. Immunofluorescence studies were conducted on cryosections of adult zebrafish hearts. These hearts were cryoprotected, mounted, sectioned, and stained as performed previously[40]. The following primary antibodies were used: anti-MHC/MF20 (mouse, Developmental Studies Hybridoma Bank, 1:100); anti-α-actinin (mouse, Diagnostic BioSystems, 1:100); anti-Raldh2 (rabbit, Abmart, 1:100); and anti–GFP (chicken, Aves Labs, 1:200). The following secondary antibodies were used: anti-mouse IgG-Alexa 405 (goat, Life technologies, 1:200), anti-mouse IgG-Alexa 594 (goat, Life Technologies, 1:200), anti-rabbit IgG-Alexa 568 (goat, Life Technologies, 1:200) and anti-chicken IgG-Alexa 488 (goat, Life Technologies, 1:200). Alexa Fluor 594-conjugated wheat germ agglutinin (Life Technologies, 50 μg ml^{-1}) was used to stain the extracellular matrix. DAPI (1 μg ml^{-1}) staining was used to identify nuclei. Notably, we discovered that eGFP from the *Tg(Tp1:eGFP)*^{um14} transgene perdured for a longer period in the ventricular outer myocardial wall (Extended Data Fig. 3) than d2GFP from the *Tg(Tp1:d2GFP)*^{mw43} transgene (Extended Data Fig. 1).

Notch signalling studies. Notch inhibition studies were performed using DAPT (a chemical inhibitor of γ-secretase) or dnMAML mis-expression (dominant negative mastermind-like 1). DAPT: zebrafish embryos were incubated in 100 μM DAPT (Sigma) or 0.1% DMSO alone (control) at specified developmental stages and time intervals and then quickly washed (two or three times) with egg water (60 μg ml^{-1} Instant Ocean sea salts) for further analysis. The ability of 100 μM DAPT treatment to inhibit Notch signalling was validated by examining *Tp1:*d2GFP expression after DAPT treatment (Extended Data Fig. 2i–p). dnMAML: The *Tg(hsp70l:dnM)* was used to globally express dnMAML at specified time points. Heat-shock induction was conducted by placing *Tg(hsp70l:dnM)* or wild-type siblings into a 37 °C incubator for 30 min, followed by 3 min in a 42 °C water bath. Embryos were heat-shocked twice every 24 h to maintain the induction of dnMAML–GFP throughout the embryo. This protocol was highly efficient at inducing dnMAML–GFP expression and produced minimal lethality. To inhibit Notch signalling in cardiomyocytes only, the *Tg(ubi:loxp-mKate2-STOP-loxp-dnMAML–GFP)* line was crossed with the *Tg(myl7:Cre)* line to produce embryos which express dnMAML–GFP only in the myocardium. Induction of dnMAML–GFP was verified by examining GFP fluorescence 5–6 h after heat shock or Cre-mediated recombination[13].

Notch activation was performed by expressing NICD. Heat shocking embryos containing both *Tg(hsp70l:loxp–mCherry–STOP-loxp-NICD-P2A–Emerald)*[14] and *Tg(myl7:Cre)* transgenes produced NICD-P2A–Emerald only in the myocardium. Heat shock was performed as described above.

Ventricular wall thickness was measured to quantify the effect of perturbing Notch signalling and was determined by drawing five representative lines perpendicular to the ventricular wall in a representative confocal slice. Thickness was measured as the distance along the line between the lateral and medial edge of the myocardial wall. All hearts were imaged in the same orientation and comparable confocal slices were chosen for analysis. Six hearts were measured for each condition.

To determine the effect of altering Notch signalling on cardiomyocyte cell numbers within the ventricular outer wall and trabecular layers, ventricular cardiomyocyte nuclei were counted from hearts exposed to specified experimental conditions using three-dimensional reconstructions of confocal slices from embryos with *myl7:*H2A–mCherry or from embryos stained with the Mef2 antibody. Mef2 immunostaining was used in embryos containing transgenes with fluorophores that overlapped with H2A–mCherry, such as *ubi:*RSdnM or *hsp70l:*RSN. For these analyses, the cells within the trabeculae could be separated from the ventricular outer wall using the post-image processing procedure described in the 'Image processing and statistical analysis' section below. Using this procedure, we calculated the number of cardiomyocyte nuclei in the total ventricle and the number of cardiomyocyte nuclei within the trabeculae. The number of cardiomyocyte nuclei in the ventricular outer wall was calculated by subtracting the number of cardiomyocytes in the trabeculae from the total.

Trabeculae area was measured from a confocal slice of a ventricle containing a cytoplasmic fluorophore such as *myl7:*mCherry or *ubi:*RSdnM or *hsp70l:*RSN. Confocal slices at the level of the AV canal were analysed. Non-trabecular tissue in these images was masked manually and then the total number of fluorescent pixels was measured using the IDL program (Research Systems). All images were taken at the same dimensions. Ventricle area was determined by measuring the total pixels outlined in the ventricle region using ImageJ software.

Clonal analysis. Cardiomyocyte clones were genetically labelled by combining the *myl7:CreER* and *priZm* (*β-act2:Brainbow1.0L*)[4] transgenes and then treating with 4-hydroxytamoxifen (4-HT, Sigma). Specifically, zebrafish embryos with these transgenes were treated at 48 hpf, when the zebrafish heart consists of a single cardiomyocyte thick wall and is looped but has not initiated cardiac trabeculation,

with 10 μM 4-HT or 0.1% ethanol (control) for 6 h at 28 °C and then washed with fresh egg water several times. The dose and length of incubation of 4-HT was titrated to create small distinct clones (one or two cells) before trabeculation (Extended Data Fig. 8). The total numbers of cardiomyocyte clones were counted from three-dimensional reconstructions of confocal slices from hearts containing *myl7:CreER* and *priZm* transgenes. Visualization and counting of clones solely within the trabeculae were analysed using the post-imaging processing procedure described in the 'Image processing and statistical analysis' section below.

Mosaic analysis by DNA injection. To create the *hsp70l:loxp–mCherry–STOP-loxp-dnSuH-P2A–Emerald* plasmid (abbreviated as *hsp70l:RSdnS*), the dominant negative Suppressor of Hairless[15] (*dnSuH*) DNA construct was PCR amplified with flanking AscI and SacII restriction sites. After sequence verification, this *dnSuH* product was subcloned into the *hsp70l:loxp–mCherry–STOP-loxp-NICD-P2A–Emerald*[14] construct (*hsp70l:RSN*), replacing the NICD sequence and generating the *hsp70l:loxp–mCherry–STOP-loxp-dnSuH-P2A–Emerald* (*hsp70l:RSdnS*) construct for subsequent injection studies (see below). To generate cardiomyocyte clones with constitutively activated or inhibited Notch signalling, the I-SceI enzyme was co-injected with either the *hsp70l:RSN* plasmid (25 pg) or the *hsp70l:RSdnS* (25 pg) plasmid into one-cell stage embryos containing *Tg(myl7:Cre; myl7:Cerulean)* or only *Tg(myl7:Cerulean)*. Embryos were then heat-shocked (as described above) at 60 hpf and imaged at 72 hpf. Cardiomyocytes containing either plasmid were detected by the co-expression of mCherry or Emerald and Cerulean. The location of Notch-altered Emerald$^+$ cardiomyocytes clones in either the ventricular outer wall or the trabeculae was determined using the method described within the 'Image processing and statistical analysis' section below.

Erbb2 and BMP loss of function studies. The activity of Erbb2, a tyrosine kinase receptor, was inhibited using (1) homozygous *erbb2*^{st50} mutants[18], (2) a splice morpholino targeting *erbb2* (*erbb2* MO)[10], or (3) the tyrosine kinase inhibitor AG1478 (Calbiochem). (1) The *erbb2*^{st50} homozygous mutant embryos were identified by the previously characterized aberrant cardiac morphology[18]. (2) The *erbb2* MO was previously characterized and shown to be specific[10]. We injected 570 pg of the *erbb2* morpholino (*erbb2* MO) or a mismatched control morpholino (control MO) into one-cell stage embryos as previously described[10]. (3) AG1478 (5 μM; Calbiochem) or 0.1% DMSO (control) was added to embryos as previously described[10]. After incubation, embryos were washed extensively with egg water for further analysis. The *erbb2* MO injections or AG1478 incubations phenocopied the *erbb2*^{st50} mutant phenotype (Fig. 3 and Extended Data Fig. 9).

To investigate the relationship between Notch signalling and *erbb2*, *erbb2* MO embryos or *erbb2*^{st50} mutant embryos were incubated with 100 μM DAPT (Sigma) or 0.1% DMSO at 60 hpf as described above. In complementary experiments, *Tg(hsp70l: dnMAML–GFP)* embryos were injected with the *erbb2* MO and heat-shocked at 60 hpf as described above.

To inhibit BMP signalling, embryos were incubated with 30 μM of Dorsomorphin (Sigma) as previously described[41]. The efficacy of Dorsomorphin was verified by examining its effect on the BMP reporter, *Tg(BRE:d2GFP)*.

Cell transplantation studies. Blastomere transplantation was performed at the mid-blastula stage as previously described[23]. Ten to twenty cells were removed from mid-blastula donor *Tg(myl7:Cerulean)* embryos and placed along the margin of either control MO or *erbb2* MO host *Tg(Tp1:d2GFP; myl7:H2A–mCherry)* embryos. Transplanted embryos in which donor cells contributed to the heart were imaged at 72 hpf. Image analysis of whether donor cells contributed to the ventricular outer wall or trabeculae and their location relative to *Tp1*:d2GFP$^+$ cells was assessed in single confocal slices or in three-dimensional reconstructions using the post-imaging procedures described within the 'Image processing and statistical analysis' section below.

***In situ* hybridization expression analyses.** Fluorescent *in situ* hybridization studies of *erbb2* and *jag2b* were performed as described in the ViewRNA *in situ* hybridization 1-Plex kit protocol (Affymetrix Panomics) with the following modifications. After the initial fixation, existing fluorescence was quenched as described for embryonic immunofluorescence above. Embryos were then subjected to protease digestion (protease QF, 1:100) at 40 °C for 30 min, followed by PBST washes and re-fixation in 4% PFA at 25 °C for 20 min. After additional PBST washes, hybridization was performed with *erbb2* probes (Affymetrix Panomics VF1-16871, 1:50 dilution) or *jag2b* probes (Affymetrix Panomics VF1-18462, 1:50 dilution) at 40 °C overnight. Hybridized embryos were then washed in PBST and stepped through pre-labelling solutions. Embryos were then incubated with label probe-AP solution (1:1,000) for 30 min at 40 °C, washed again, transferred to a AP-enhancer solution and then transferred to fast red solution (one fast red substrate tablet in 5 ml naphthol buffer) for 30 min at 40 °C. After PBST washes, embryos were incubated in anti-MHC/MF20 antibody (mouse, Developmental Studies Hybridoma Bank, 1:100) or anti–GFP antibody (chicken, Aves Labs, 1:200) overnight at 4 °C. After PBST washes, embryos were incubated in anti-mouse IgG-Alexa 488 (goat, Life Technologies, 1:200) or anti-chicken IgG-Alexa 488 antibodies (goat, Life Technologies, 1:200) for 1 h at 25 °C. Finally, embryos were washed and mounted for imaging. PBST washing consisted of three washes for 15 min each at 25 °C. For *gfp* mRNA expression analysis, wholemount *in situ* hybridization studies were performed as previously described[40].

Image processing and statistical analysis. All images were obtained using a Nikon C2 confocal microscope and processed using Nikon NIS Elements software and ImageJ as previously described[40]. Scale bars for all images represent 25 μm. Measurements comparing the ventricular outer wall with the trabeculae were performed with post-image processing of confocal slices. Visualization of all cardiomyocytes and clones within the ventricle (comprising both the ventricular outer wall and the trabeculae) were made using three-dimensional reconstructions (Nikon NIS Elements) of confocal slices. However, to visualize only the trabeculae, cardiomyocytes within the ventricular outer wall in individual confocal slices were identified by their outer location and orientation and then masked manually. Three-dimensional reconstructions with these masked confocal slices then allowed the visualization and measurement of trabeculae alone. Measurements for the ventricular outer wall alone were calculated by subtracting the measurements of the trabeculae from the total ventricular cardiomyocytes. No statistical methods were used to predetermine sample size. Animals were assigned to experimental groups using simple randomization, without investigator blinding. Unpaired two-tailed Student's *t*-tests or Fisher's exact tests were used to determine statistical significance. $P < 0.05$ was considered to be statistically significant, as indicated by an asterisk. Error bars, s.e.m.

30. Chi, N. C. *et al.* Foxn4 directly regulates tbx2b expression and atrioventricular canal formation. *Genes Dev.* **22,** 734–739 (2008).
31. Palencia-Desai, S. *et al.* Vascular endothelial and endocardial progenitors differentiate as cardiomyocytes in the absence of Etsrp/Etv2 function. *Development* **138,** 4721–4732 (2011).
32. D'Amico, L., Scott, I. C., Jungblut, B. & Stainier, D. Y. A mutation in zebrafish hmgcr1b reveals a role for isoprenoids in vertebrate heart-tube formation. *Curr. Biol.* **17,** 252–259 (2007).
33. Kikuchi, K. *et al.* Primary contribution to zebrafish heart regeneration by gata4$^+$ cardiomyocytes. *Nature* **464,** 601–605 (2010).
34. Kettleborough, R. N. *et al.* A systematic genome-wide analysis of zebrafish protein-coding gene function. *Nature* **496,** 494–497 (2013).
35. Huang, C. J., Tu, C. T., Hsiao, C. D., Hsieh, F. J. & Tsai, H. J. Germ-line transmission of a myocardium-specific GFP transgene reveals critical regulatory elements in the cardiac myosin light chain 2 promoter of zebrafish. *Dev. Dyn.* **228,** 30–40 (2003).
36. Thermes, V. *et al.* I-SceI meganuclease mediates highly efficient transgenesis in fish. *Mech. Dev.* **118,** 91–98 (2002).
37. Mosimann, C. *et al.* Ubiquitous transgene expression and Cre-based recombination driven by the ubiquitin promoter in zebrafish. *Development* **138,** 169–177 (2011).
38. Kwan, K. M. *et al.* The Tol2kit: a multisite gateway-based construction kit for Tol2 transposon transgenesis constructs. *Dev. Dyn.* **236,** 3088–3099 (2007).
39. Zhou, Y. *et al.* Latent TGF-β binding protein 3 identifies a second heart field in zebrafish. *Nature* **474,** 645–648 (2011).
40. Zhang, R. *et al.* In vivo cardiac reprogramming contributes to zebrafish heart regeneration. *Nature* **498,** 497–501 (2013).
41. Yu, P. B. *et al.* Dorsomorphin inhibits BMP signals required for embryogenesis and iron metabolism. *Nature Chem. Biol.* **4,** 33–41 (2008).

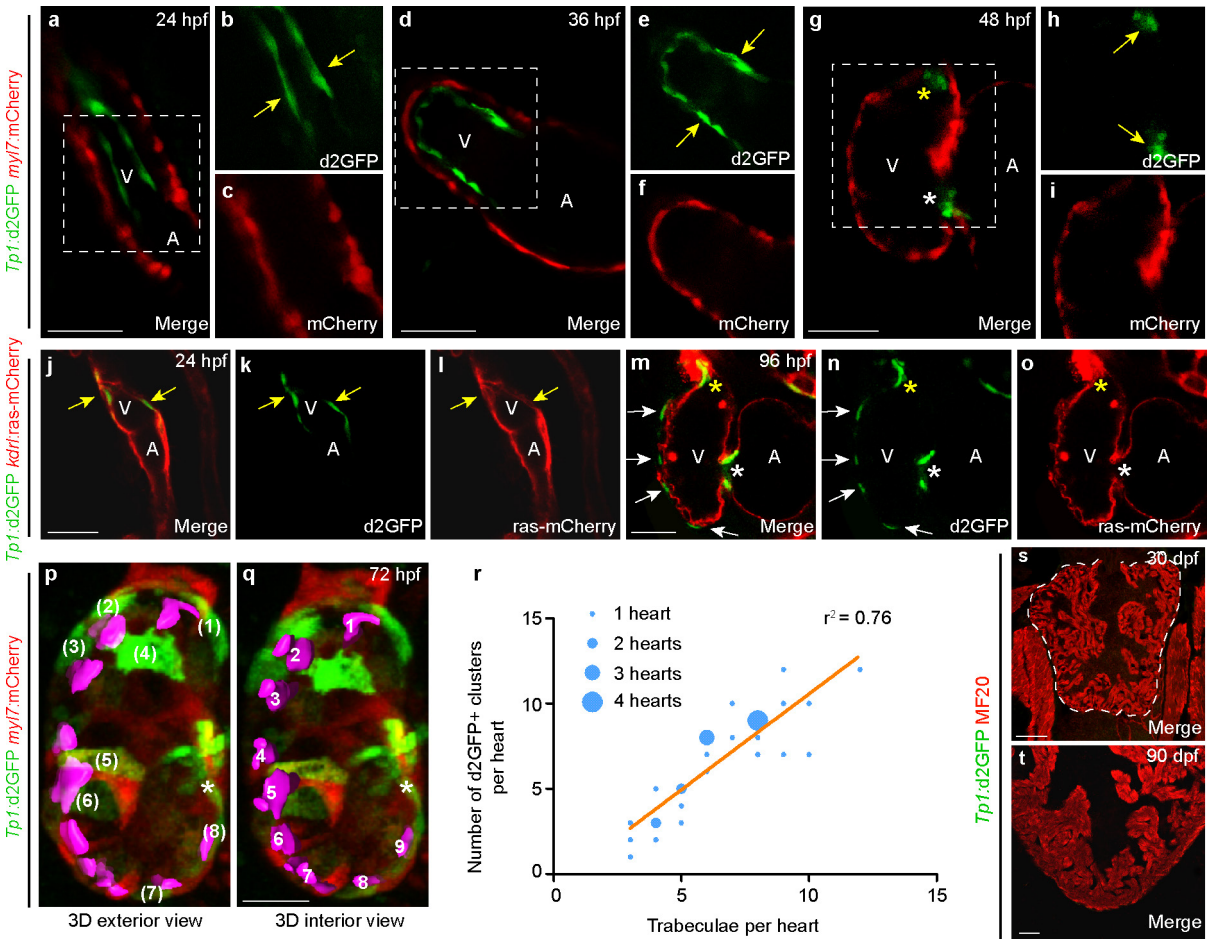

Extended Data Figure 1 | Notch signalling is dynamically activated in the endocardium and myocardium during heart development. **a**–**f**, Confocal slices of *Tg(Tp1:d2GFP; myl7:mCherry)* hearts reveal that Notch signalling is in the ventricular endocardium (yellow arrows) but not in the myocardium at 24 hpf ($n = 11$) and 36 hpf ($n = 8$), but (**g**–**i**) becomes restricted to the AV and OFT endocardium by 48 hpf ($n = 12$). **j**–**o**, *Tg(Tp1:d2GFP; kdrl:ras–mCherry)* confocal imaging confirms that *Tp1*:d2GFP is expressed in the ventricular endocardium at (**j**–**l**) 24 hpf ($n = 8$) but becomes localized to the AV or OFT endocardium as well as non-endocardial cells in the outer ventricular myocardial wall (white arrows) by (**m**–**o**) 96 hpf ($n = 10$). **p**, **q**, Three-dimensional confocal reconstructions of the (**p**) exterior and (**q**) interior regions of 72 hpf *Tg(Tp1:d2GFP; myl7:mCherry)* hearts reveal that Notch-activated *Tp1*:d2GFP$^+$ cells are present in cardiomyocyte clusters (green, numbers in parentheses) and excluded from nascent cardiac trabeculae (pseudo-colour magenta, numbers). **r**, Graph shows that the number of cardiac trabeculae (*x* axis) and *Tp1*:d2GFP$^+$ cardiomyocyte clusters (*y* axis) are similar within the ventricle ($n = 30$) at 72 hpf. Size of dots indicates the number of embryos with a particular number of trabeculae and *Tp1*:d2GFP$^+$ clusters. Line represents a linear regression fitted to the data. **s**, **t**, Myocardial anti-MHC/MF20 immunostaining of *Tg(Tp1:d2GFP)* hearts reveals a loss of myocardial *Tp1*:d2GFP Notch reporter signal at 30 and 90 dpf hearts ($n = 5$ hearts per stage). White arrows, likely *Tp1*:d2GFP$^+$ cardiomyocytes; yellow arrows, *Tp1*:d2GFP$^+$ endocardial cells; white and yellow asterisks, AV and OFT. Dashed line in **s** outlines ventricle. V, ventricle; A, atrium. Scale bar, 25 μm.

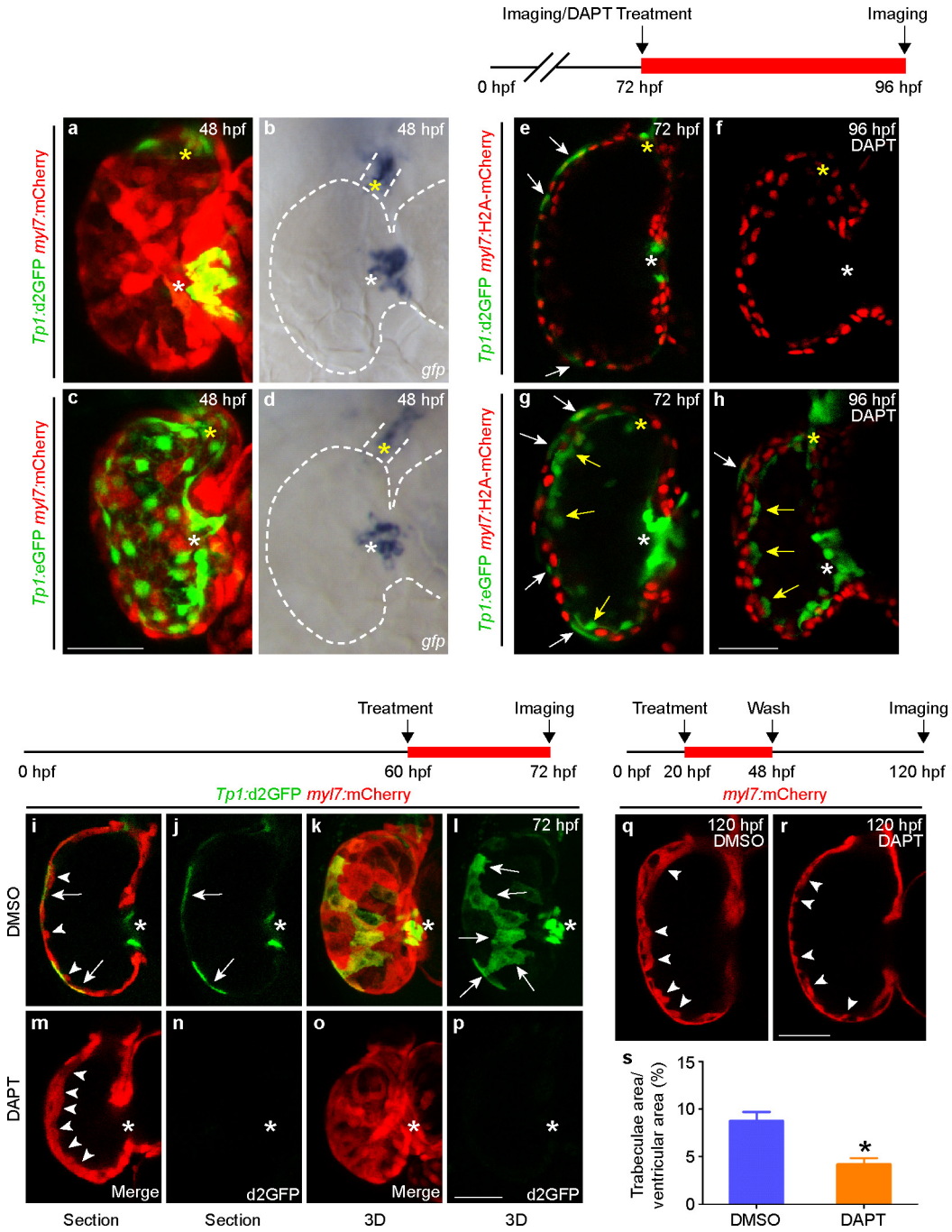

Extended Data Figure 2 | DAPT treatment validates that the Notch reporter *Tp1*:d2GFP monitors dynamic Notch signalling more closely than *Tp1*:eGFP, and reveals opposing roles of Notch signalling on trabeculation at different developmental stages. a–d, At 48hpf, (**a**) *Tp1*:d2GFP expression is restricted to the AV and OFT endocardium ($n = 8/8$ embryos) whereas (**c**) *Tp1*:eGFP is expressed in the ventricular, AV and OFT endocardium ($n = 6/6$). However, *gfp* mRNA is primarily expressed in the AV and OFT regions in both (**b**) *Tg(Tp1:d2GFP; myl7:mCherry)* ($n = 10/10$) and (**d**) *Tg(Tp1:eGFP; myl7:mCherry)* embryos ($n = 5/5$), revealing that *Tp1*:d2GFP expression most closely matches Notch reporter activity. **e–h**, After 24 h DAPT treatments of (**e**, **f**) *Tg(Tp1:d2GFP; myl7:H2A–mCherry)* and (**g**, **h**) *Tg(Tp1:eGFP; myl7:H2A–mCherry)* embryos at 72 hpf, (**f**) *Tp1*:d2GFP is more diminished throughout the heart at 96 hpf ($n = 8/10$) compared with (**h**) *Tp1*:eGFP ($n = 6/7$), confirming *Tp1*:d2GFP signal more faithfully recapitulates Notch signalling dynamics. **m–p**, *Tg(Tp1:d2GFP; myl7:mCherry)* hearts DAPT-treated from 60 to 72 hpf exhibit increased trabeculation (white arrowheads) and diminished *Tp1*:d2GFP Notch reporter activity ($n = 12/16$) than (**i–l**) DMSO-treated hearts ($n = 0/20$). However, (**r**) *Tg(myl7:mCherry)* hearts DAPT-treated from 20 to 48 hpf exhibit reduced trabeculae at 120 hpf ($n = 12/15$) than (**q**) DMSO-treated hearts ($n = 0/20$). **s**, Graph represents trabeculae/total ventricular area in embryos treated with DMSO or DAPT in **q** and **r**. White and yellow arrows, myocardial and endocardial Notch reporter activity; white arrowheads, trabeculae; white and yellow asterisks, AV and OFT. Scale bar, 25 μm. Mean ± s.e.m. $^*P < 0.05$ by Student's *t*-test.

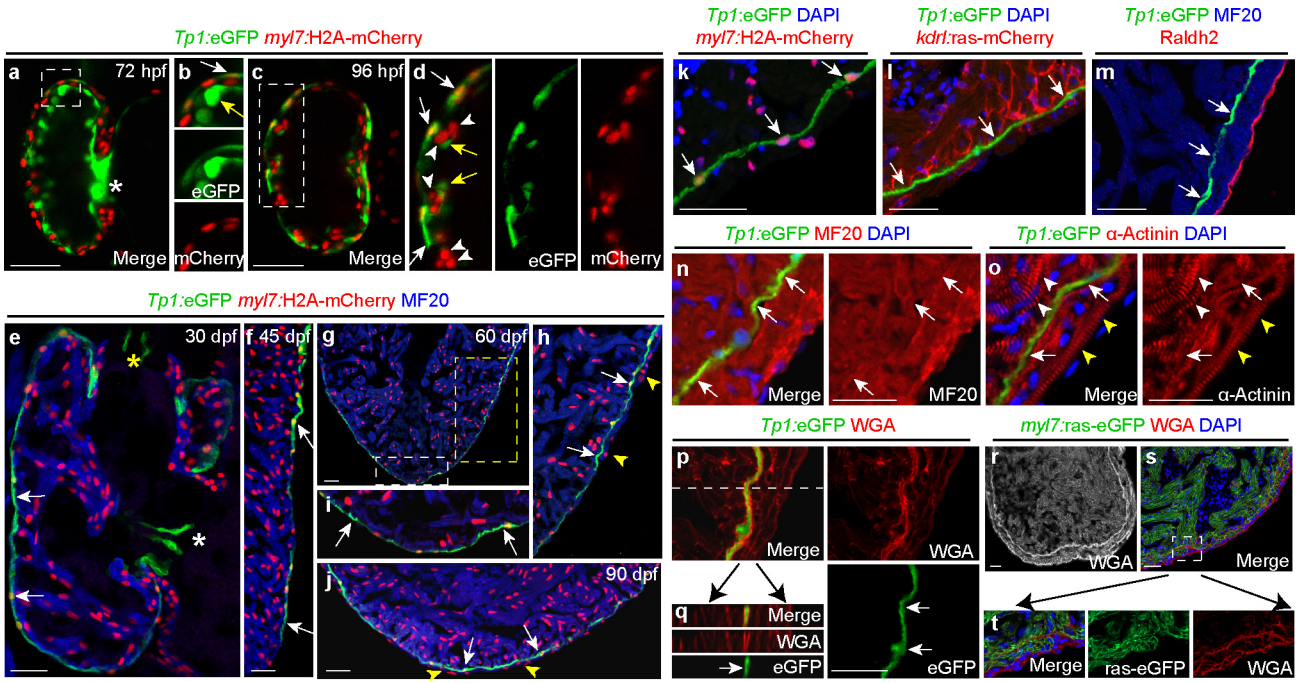

Extended Data Figure 3 | *Tp1*:eGFP labels the ventricular outer wall during early cardiac development, which becomes the distinctive ventricular primordial myocardium in adults. Using the *Tp1*:eGFP Notch reporter, which exhibits greater fluorescence perdurance than *Tp1*:d2GFP, we performed limited fate mapping of Notch activated cardiac cells during ventricular morphogenesis. **a**, **b**, *Tp1*:eGFP is expressed not only in ventricular cardiomyocytes (red nuclei, white arrows) at 72 hpf but also throughout the ventricular endocardium because of eGFP perdurance (yellow arrows) ($n = 12$). **c**, **d**, Although diminishing in the ventricular endocardium (yellow arrows) at 96 hpf ($n = 14$), *Tp1*:eGFP expands in the outer ventricular myocardial wall (white arrows), yet is notably absent from myocardial trabeculae (white arrowheads). **e**, **f**, By 30 and 45 dpf ($n = 6$, $n = 5$), *Tp1*:eGFP remains in the peripheral ventricular (primordial) myocardial layer, which is one cardiomyocyte thick (*myl7*:H2A–mCherry$^+$/red and MF20$^+$/blue), but is reduced in the ventricular but not the AV or OFT endocardium. **g**–**i**, At 60 dpf ($n = 5$), (**h**) new cardiomyocytes (cortical layer, yellow arrowheads) form over the *Tp1*:eGFP$^+$ primordial myocardium (white arrows) at the ventricular myocardial base (yellow box in **g**) and extend towards the apex where (**i**)*Tp1*:eGFP$^+$ cardiomyocytes (white arrows) still remain the outer most layer of the ventricular myocardium (white box in **g**). **j**, However, by 90 dpf ($n = 5$), this new cortical myocardial layer (yellow arrowheads) spreads over the apical *Tp1*:eGFP$^+$ ventricular primordial myocardium (white arrows). **k**–**m**, In adult hearts (90 dpf), *Tp1*:eGFP is primarily found in the (**k**, $n = 5$) *myl7*:H2A–mCherry$^+$ primordial myocardium but not in the (**l**, $n = 5$) endocardium marked by *kdrl*:ras–mCherry, nor (**m**, $n = 3$) epicardium marked by Raldh2 localization. **n**–**t**, Adult hearts (6 months) were further examined to assess the cellular attributes of the primordial layer. **n**, Anti-MHC/MF20 immunostaining confirms that *Tp1*:eGFP$^+$ cardiac cells are myocardial ($n = 5$). **o**, Anti-α-actinin immunostaining reveals that trabecular (white arrowheads) and cortical (yellow arrowheads) cardiomyocytes display organized sarcomeric structures but the *Tp1*:eGFP$^+$ primordial cardiomyocytes (arrows) do not ($n = 7$). **p**–**t**, Wheat germ agglutinin (WGA) staining shows that (**p**, **q**) the *Tp1*:eGFP$^+$ primordial myocardial layer is surrounded by extensive extracellular matrix ($n = 5$) and that (**r**–**t**) *Tg(myl7:ras–eGFP)* primordial cardiomyocytes display a thin cellular morphology compared with other ventricular cardiomyocytes ($n = 10$). **q**, An *X*–*Z* reconstruction of confocal stacks from *Tp1*:eGFP and wheat germ agglutinin stainings at the dashed line shown in **p**. **b**, **d**, **h**–**i**, **t**, Magnifications of the boxed areas in **a**, **c**, **g**, **s**, respectively. White and yellow arrows, myocardial and endocardial *Tp1*:eGFP; white and yellow arrowheads, trabeculae and cortical layer; white and yellow asterisks, AV and OFT. Scale bar, 25 μm.

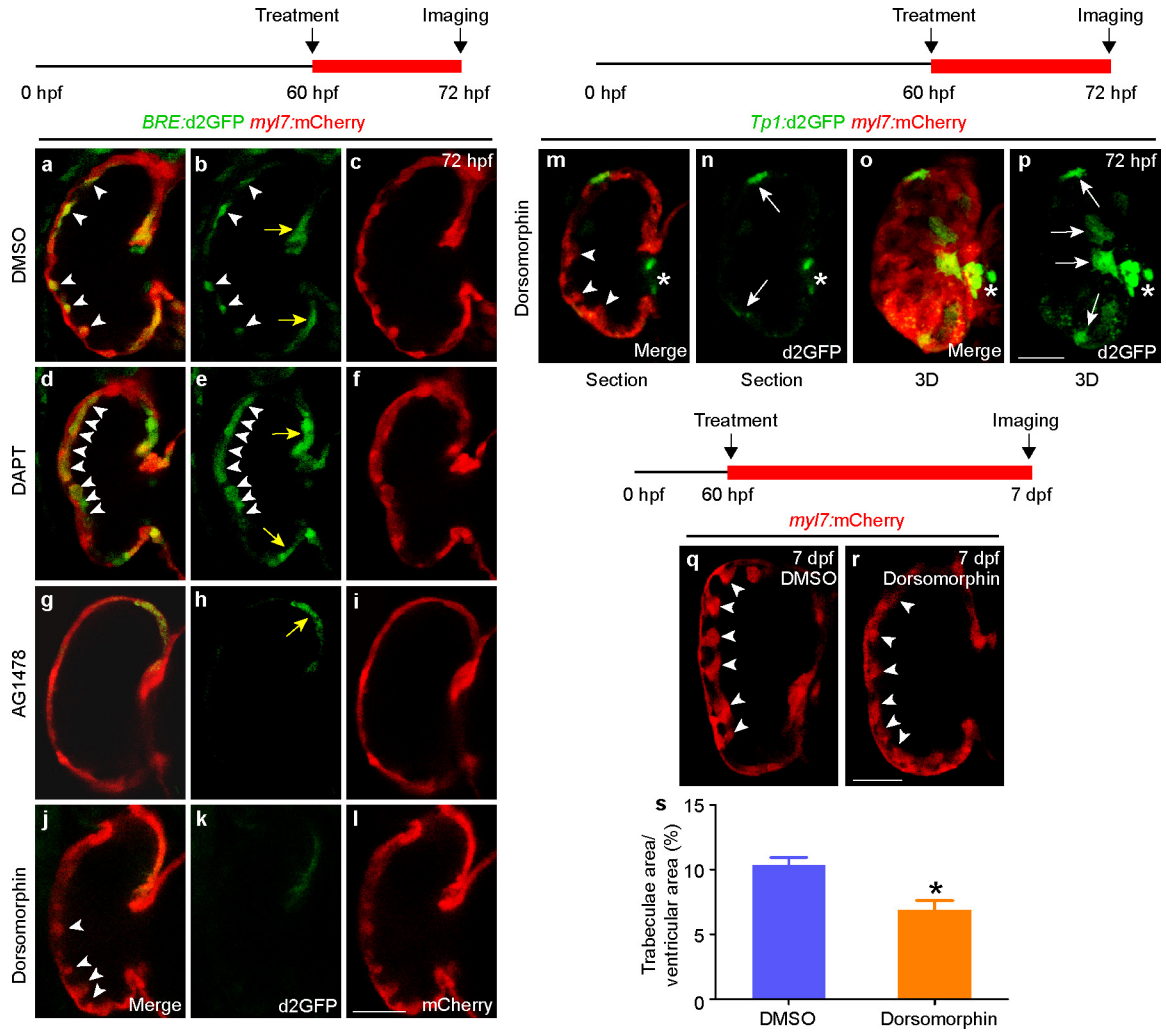

Extended Data Figure 4 | BMP signalling, which marks trabeculae, is required for expanding but not initiating trabeculae formation and has no effect on myocardial Notch activity. a–l, *Tg(BRE:d2GFP; myl7:mCherry)* hearts were treated with (**a–c**) DMSO, (**d–f**) DAPT, (**g–i**) AG1478, or (**j–l**) Dorsomorphin at 60 hpf and imaged at 72 hpf. **a–c**, DMSO-treated hearts express the *BRE:*d2GFP BMP reporter in trabeculae (arrowheads) and in the AV myocardium (yellow arrows, $n = 11/11$ embryos). **d–f**, DAPT-treated hearts exhibit increased trabeculation and *BRE:*d2GFP expression in these forming trabeculae (arrowheads, $n = 9/12$). **g–i**, AG1478-treated hearts fail to form trabeculae ($n = 9/10$) and only express the *BRE:*d2GFP BMP reporter in the AV myocardium (yellow arrow). **j–l**, Dorsomorphin-treated hearts form cardiac trabeculae (arrowheads) but fail to express the *BRE:*d2GFP BMP reporter in both cardiac trabeculae and the AV myocardium ($n = 10/12$). **m–p**, Treating *Tg(Tp1:d2GFP; myl7:mCherry)* embryos with Dorsomorphin from 60 to 72 hpf did not affect the initiation of trabeculae (arrowheads) nor the activation of myocardial Notch signalling (white arrows, $n = 13/16$) compared with treating with DMSO (see Extended Data Fig. 2i–l). **q**, **r**, Although *Tg(myl7:mCherry)* hearts treated with (**q**) DMSO or (**r**) Dorsomorphin from 60 hpf to 7 dpf form similar numbers of trabeculae (arrowheads), Dorsomorphin-treated hearts display trabeculae that are stunted/reduced in size ($n = 12/15$) compared with DMSO-treated control hearts ($n = 0/15$). **s**, Graph reveals a significant reduction in the trabecular/ventricular area ratio in Dorsmorphin-treated fish compared with DMSO-treated controls. Arrowheads, trabeculae; yellow arrows, AV myocardium; white arrows, *Tp1*:d2GFP$^+$ myocardium. White asterisks, AV. Mean ± s.e.m. $^*P < 0.05$ by Student's *t*-test. Scale bar, 25 μm.

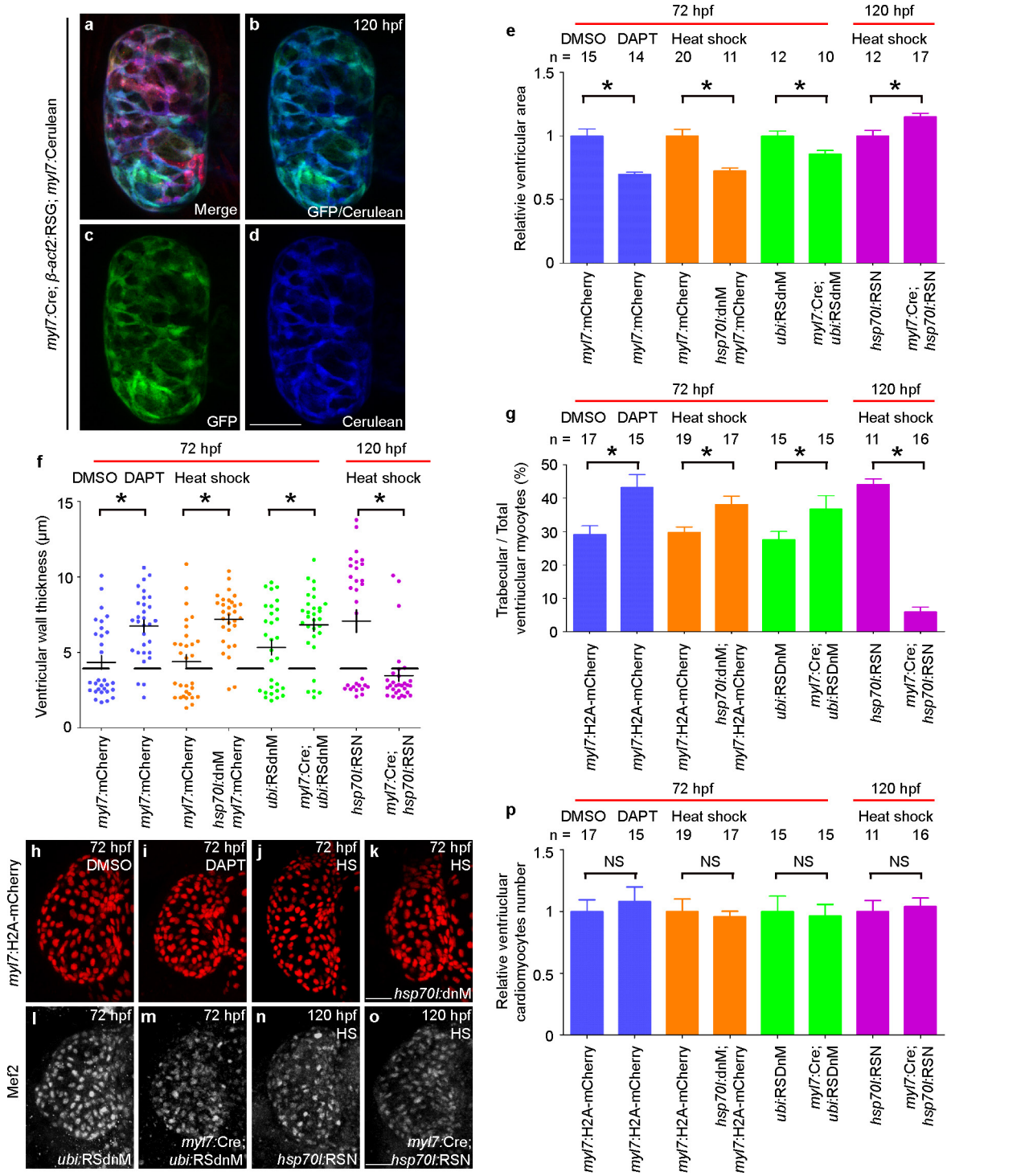

Extended Data Figure 5 | Altering myocardial Notch signalling affects ventricular size and wall thickness but not total number of ventricular cardiomyocytes. a–d, The *Tg(myl7:Cre)* transgenic line used to specifically perturb Notch signalling in the myocardium was validated by confirming that Cre expression is restricted to the myocardium. Activity of *myl7*:Cre, as visualized by (**c**) GFP expression from the switch line, *β-act2*:RSG, exclusively overlaps with (**b**, **d**) *myl7*:Cerulean expression at 120 hpf ($n = 10$ embryos). Quantitative analyses of (**e**) ventricular size and (**f**) wall thickness performed on confocal images from Fig. 2a–h reveal that myocardial Notch signalling restricts ventricular size while promoting ventricular wall thickness. **e**, Ventricular size measurements were normalized to respective controls for each condition. **f**, Individual measurements (dots) of myocardial thickness were taken across the outer curvature of the ventricle ($n = 30$ measurements, 6 measurements were taken per embryo, 5 embryos per condition). Dashed line represents the ventricular wall thickness that distinguishes trabeculated myocardial thickness from ventricular outer wall myocardial thickness in control hearts. Crosses denote mean and s.e.m. **g–p**, Quantitative analysis of (**g**) trabecular cardiomyocytes and (**p**) total ventricular cardiomyocytes was calculated by counting myocardial nuclei labelled with *myl7*:H2A–mCherry or anti-Mef2 immunostaining using embryos from Fig. 2i–p for **g**, or from three-dimensional reconstructions in **h–o** for **p**. In **g**, the number of trabecular/total ventricular cardiomyocytes was used to calculate the percentage of trabecular cardiomyocytes for each condition. In **p**, total ventricular cardiomyocytes were normalized to respective controls for each condition. *n*, Number of embryos analysed per condition. Mean ± s.e.m. $^*P < 0.05$ by Student's *t*-test. NS, not significant. Scale bar, 25 μm.

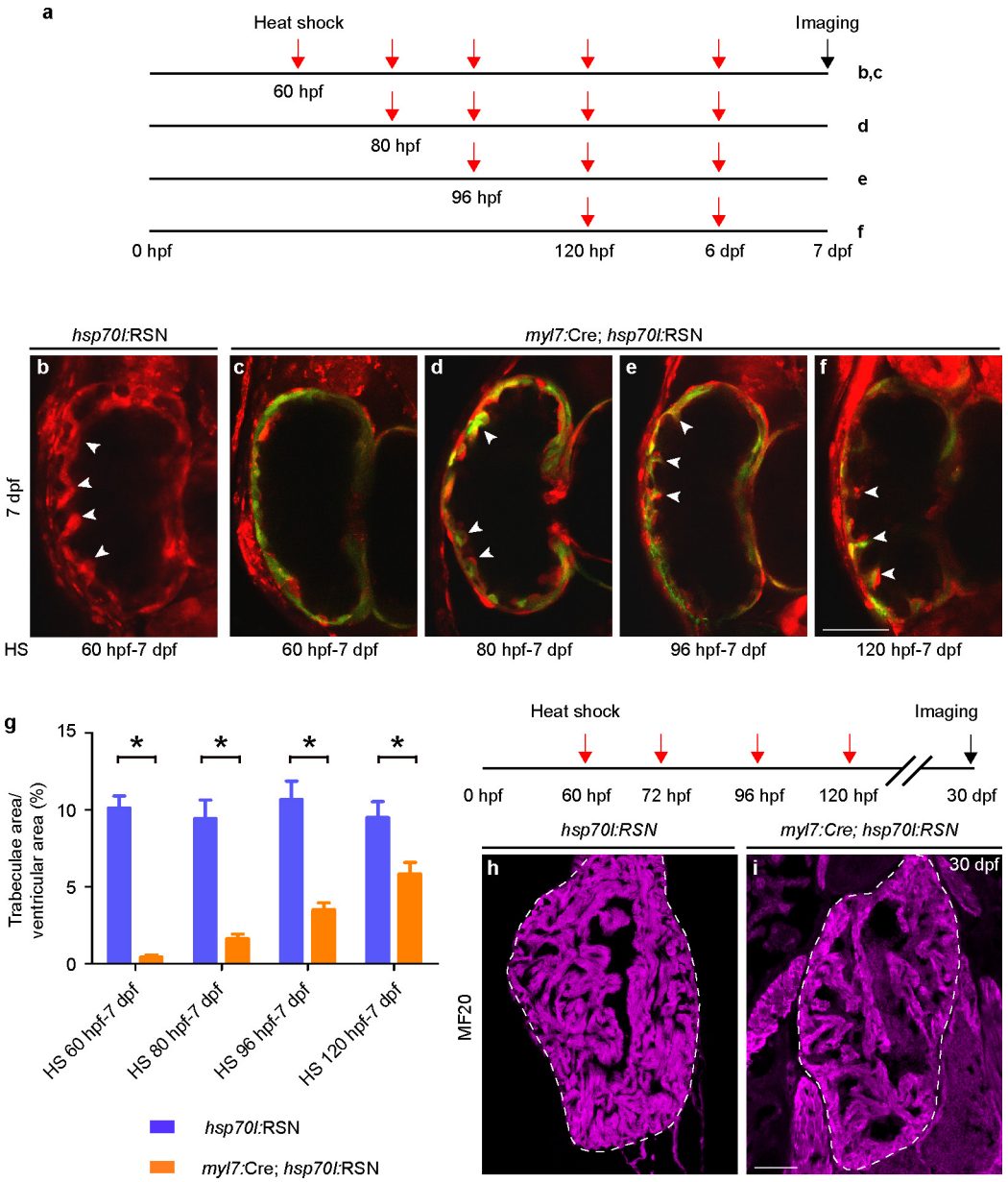

Extended Data Figure 6 | Myocardial Notch activation can inhibit the formation and expansion of cardiac trabeculae at various cardiac developmental stages. a–g, *Tg(myl7:Cre; hsp70l:RSN)* and *Tg(hsp70l:RSN)* (control) embryos were heat-shocked (HS) during various developmental time windows as indicated and imaged at 7 dpf to assess the effects of constitutive myocardial Notch signalling on cardiac trabeculae formation. **a**, Red arrows in schematic indicate the time points at which embryos in the corresponding panels were heat-shocked. **b**, Control *Tg(hsp70l:RSN)* embryos heat-shocked from 60 hpf to 7 dpf ubiquitously express mCherry but do not overexpress myocardial NICD. They form cardiac trabeculae (arrowheads) similar to wild-type embryos (control, $n = 14/15$). **c**, However, *Tg(myl7:Cre; hsp70l:RSN)* embryos heat-shocked from 60 hpf to 7 dpf overexpress NICD-P2A–Emerald throughout the myocardium and fail to form cardiac trabeculae ($n = 9/12$). Although *Tg(myl7:Cre; hsp70l:RSN)* embryos heat-shocked at (**d**) 80 hpf, (**e**) 96 hpf, and (**f**) 120 hpf form trabeculae, these embryos exhibit stunted/smaller trabeculae after heat-shocking ($n = 9/10$, 10/14, and 12/16, respectively). **g**, Graph of trabeculae/total ventricular area of heat-shocked embryos from **b**–**f**, showing that myocardial Notch over-activation inhibits the progression of cardiac trabeculae formation. **h**, **i**, Although heat-shocking *Tg(myl7:Cre; hsp70l:RSN)* from 60 to 120 hpf initially inhibits trabeculae formation, (**i**) the ventricular myocardium (detected by anti-MHC/MF20 immunostaining, magenta) can still form trabeculae, albeit at reduced numbers ($n = 4/5$) by 30 dpf after stopping NICD overexpression compared with (**h**) heat-shocked *Tg(hsp70l:RSN)* hearts (control, $n = 0/8$). HS, heat-shock; white arrowheads, trabeculae. Scale bar, 25 μm. Mean ± s.e.m. $^*P < 0.05$ by Student's *t*-test.

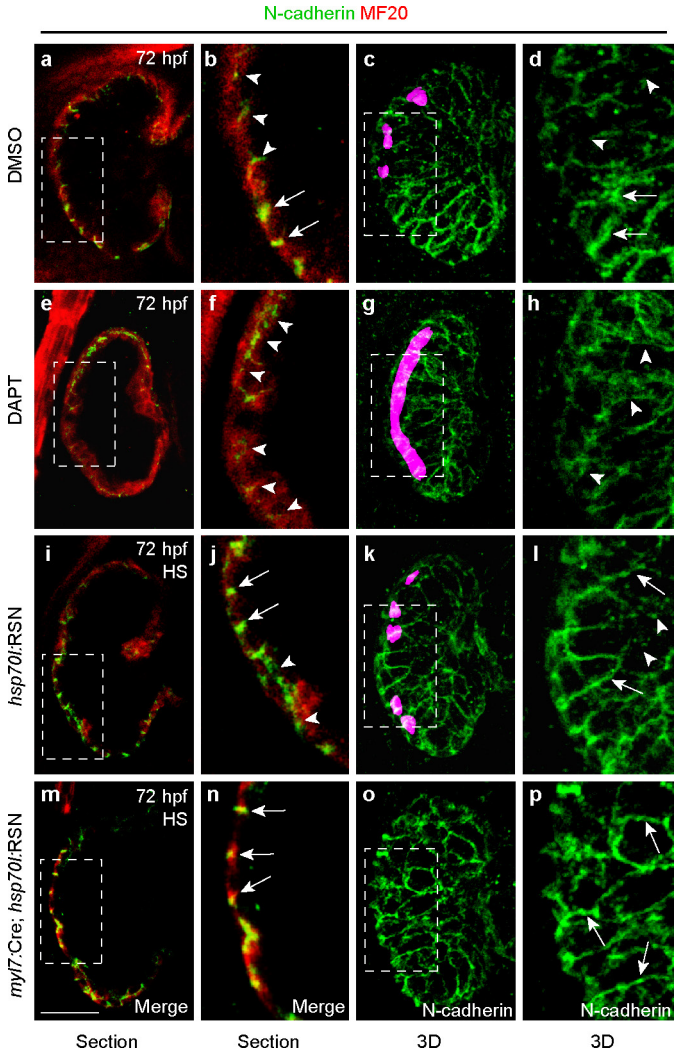

Extended Data Figure 7 | Notch signalling regulates cardiomyocyte cell junctions during cardiac trabeculae formation. a–d, In DMSO-treated (control) 72 hpf wild-type hearts, N-cadherin is localized at cell junctions of cardiomyocytes within the ventricular outer wall (arrows) but redistributes away from these cell–cell contacts in cardiomyocytes that extend into the lumen to form trabeculae (arrowheads) ($n = 12/12$). **e–h**, Notch inhibition by DAPT treatment promotes N-cadherin redistribution and results in increased trabeculation ($n = 8/11$). **m–p**, Conversely, myocardial Notch activation by heat shocking (HS) *Tg(myl7:Cre; hsp70l:RSN)* leads to diminished N-cadherin redistribution and reduced trabeculation ($n = 7/10$) compared with (**i–l**) heat-shocked *Tg(hsp70l:RSN)* control hearts ($n = 0/10$). Nascent cardiac trabeculae were pseudo-coloured magenta in **c**, **g** and **k**. **b**, **d**, **f**, **h**, **j**, **l**, **n**, **p**, Magnifications of boxed areas in **a**, **c**, **e**, **g**, **i**, **k**, **m**, **o**, respectively. Arrowheads, N-cadherin redistributed from cell–cell contacts; arrows, N-cadherin at cell–cell contacts within outer wall. Scale bar, 25 μm.

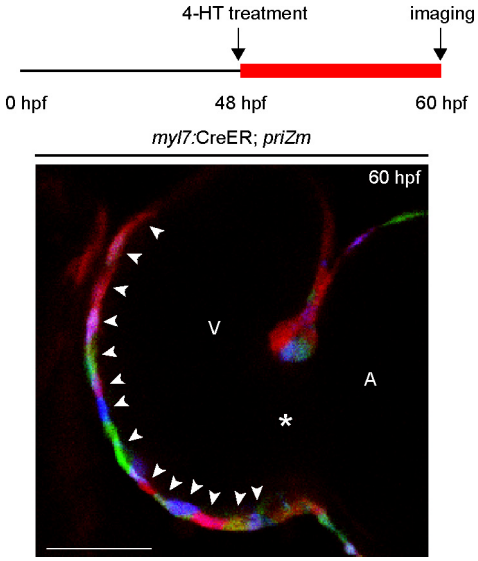

Extended Data Figure 8 | Tamoxifen treatment of *Tg(myl7:CreER; priZm)* embryos at 48 hpf labels adjacent individual cardiomyocytes with combinations of distinct fluorescent colours. *Tg(myl7:CreER; priZm)* embryos were treated with 4-HT at 48 hpf and confocal imaged at 60 hpf before the initiation of cardiomyocytes forming trabeculae. Individual cardiomyocytes (arrowheads) are labelled with distinct combinations of fluorescent proteins allowing for tracking of specific cardiomyocyte clones ($n = 6$). White arrowheads, cardiomyocytes; V, ventricle; A, atrium; white asterisk, AV. Scale bar, 25 μm.

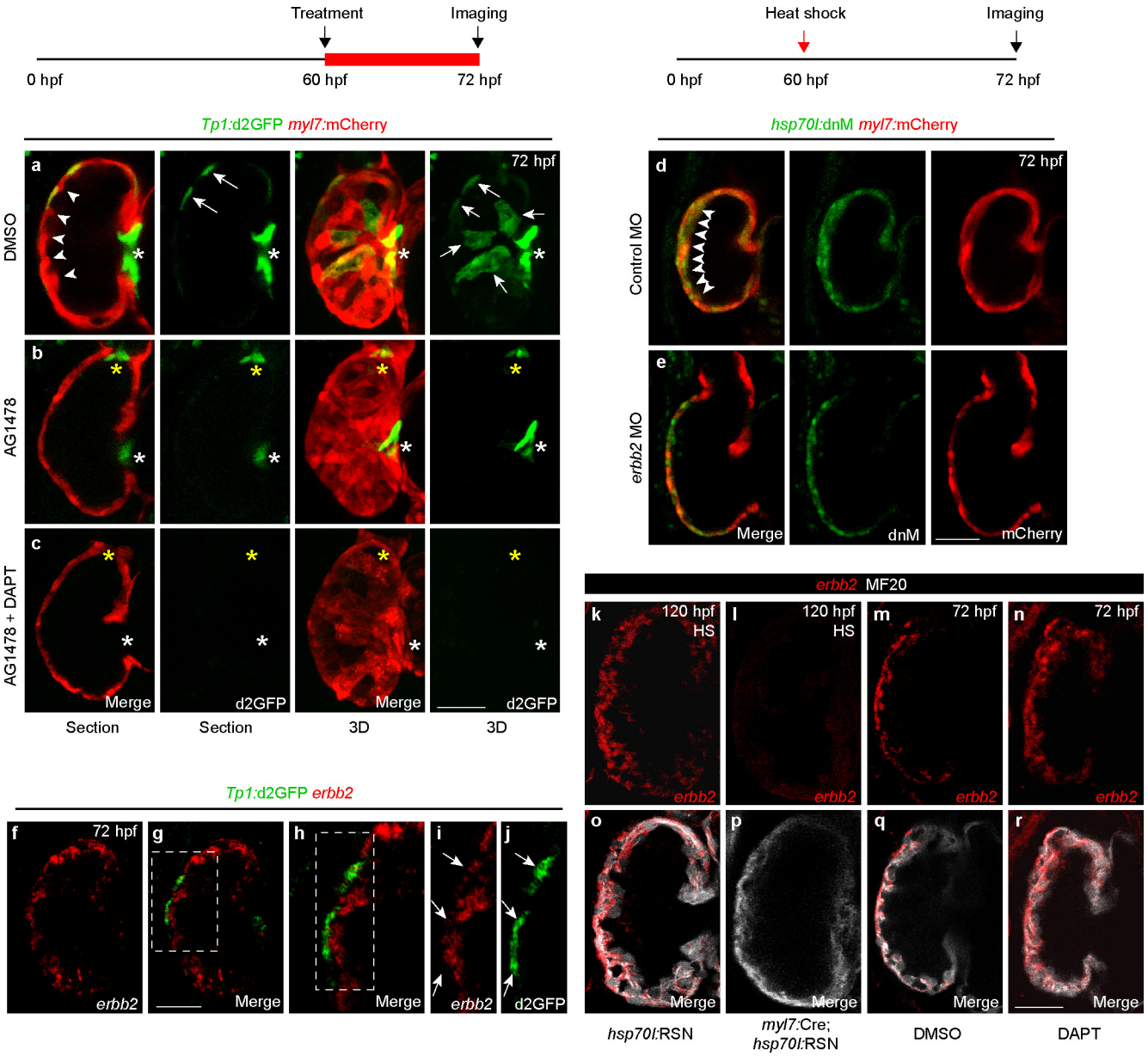

Extended Data Figure 9 | Notch and Erbb2 signalling pathways form a feedback loop during cardiac trabeculation. a, **b**, Compared with (**a**) DMSO-treated *Tg(Tp1:d2GFP; myl7:mCherry)* (controls) embryos, (**b**) inhibiting Erbb2 function with AG1478 from 60 to 72 hpf blocks trabeculation and myocardial Notch signalling ($n = 14/17$), confirming *erbb2* MO and mutant phenotypes. **c**, However, Notch inhibition using DAPT cannot reverse the AG1478/Erbb2 inhibition effect on trabeculae formation ($n = 11/12$). **d**, **e**, Consistent with these results, (**d**) control MO-injected *Tg(hsp70l:dnM; myl7:mCherry)* embryos expressing heat-shock induced dnMAML from 60 to 72 hpf display increased trabeculation (arrowheads, $n = 9/11$); (**e**) however, *erbb2* MO-injected embryos expressing heat-shock induced dnMAML fail to display trabeculae ($n = 9/12$) as similarly observed in *erbb2* MO-injected embryos alone (Fig. 3). **f**–**j**, The *erbb2* fluorescent *in situ* hybridization and GFP co-immunostaining performed on 72 hpf *Tg(Tp1:d2GFP)* hearts reveal that *erbb2* is expressed in an intermittent pattern across the ventricular wall and is specifically diminished in *Tp1*:d2GFP$^+$ cells (arrows) ($n = 6/6$). **l**, **p**, Heat-shocked (HS) *Tg(myl7:Cre; hsp70l:RSN)* hearts, which exhibit constitutively activated myocardial Notch signalling (NICD) from 60 to 120 hpf, minimally express *erbb2* in the myocardium ($n = 8/11$) compared with (**k**, **o**) heat-shocked *Tg(hsp70l:RSN)* control hearts ($n = 0/20$) at 120 hpf. Compared with (**m**, **q**) DMSO-treated control hearts ($n = 0/10$), (**n**, **r**) Notch-inhibited hearts by DAPT treatment from 60 to 72 hpf exhibit increased myocardial *erbb2* expression as well as more trabeculae at 72 hpf ($n = 8/10$), supporting the idea that Notch signalling inhibits *erbb2* expression. **h**, **i**–**j**, Magnifications of boxed areas in **g**, **h**, respectively. Arrowheads, trabeculae; arrows, *Tp1*:d2GFP$^+$ cardiomyocytes; white and yellow asterisks, AV and OFT. Scale bar, 25 μm.

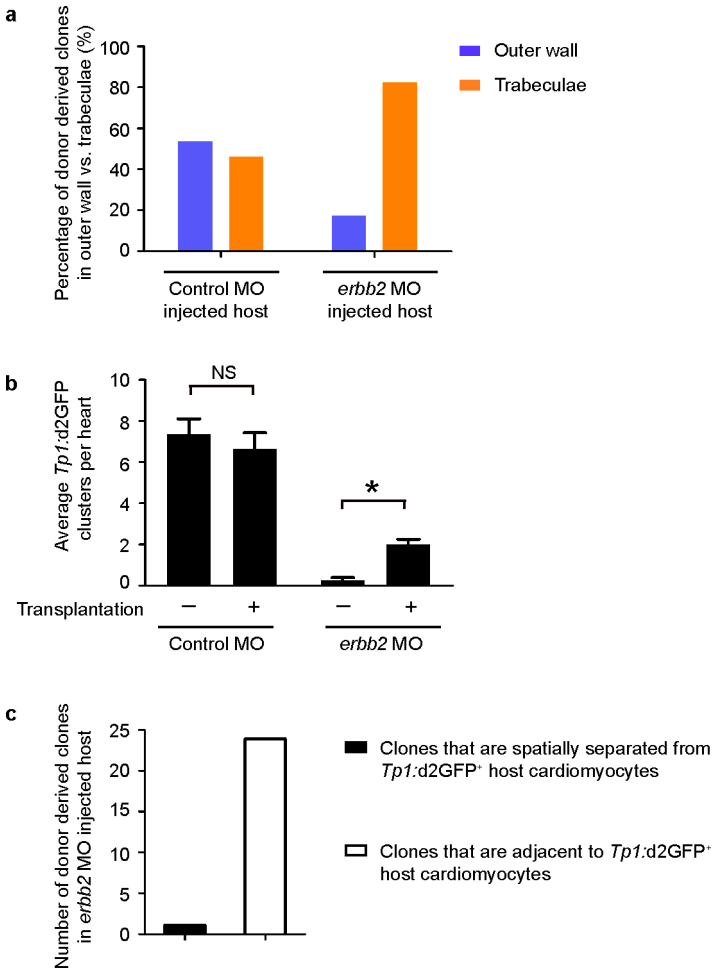

Extended Data Figure 10 | Transplanted wild-type cardiomyocytes non-cell-autonomously activate Notch signalling in *erbb2* morphant host cardiomyocytes. a, On the basis of mosaic embryo studies from Fig. 3f–i, wild-type donor cardiomyocytes contribute equally to the outer ventricular wall (14/26 clones) or the trabeculae (12/26 clones) when transplanted into control MO host embryos ($n = 12$ embryos). However, when wild-type donor cells are transplanted into *erbb2* MO host embryos ($n = 10$ embryos), they contribute more to the trabecular layer (19/23 clones) than to the ventricular outer wall (4/23 clones, $P < 0.05$ by Fisher's exact test). **b**, On the basis of mosaic embryo studies from Fig. 3f–i, transplanting wild-type donor cells increases the number of *erbb2* MO host cardiomyocytes expressing *Tp1*:d2GFP ($n = 10$ embryos) compared with non-transplanted *erbb2* MO embryos ($n = 16$ embryos), but had no effect on the number of control MO host cells expressing *Tp1*:d2GFP ($n = 12$ embryos) compared with non-transplanted controls ($n = 11$ embryos). **c**, Quantitative data for Fig. 3f–i reveal that transplanted wild-type donor cardiomyocytes are primarily adjacent to host *Tp1*:d2GFP$^+$ cardiomyocytes in *erbb2* MO hearts ($n = 10$ embryos). Mean ± s.e.m. *$P < 0.05$ by Student's *t*-test. NS, not significant.